POLITECNICO DI TORINO

MECHANICAL AND AEROSPACE ENGINEERING DEPARTMENT

Master degree course in Aerospace Engineering

Master Degree Thesis

Methodology and tools for propulsive performance characterization of high-speed aircraft in conceptual design

Supervisors
Prof.ssa Nicole Viola
Dr. Davide Ferretto
Dr. Roberta Fusaro

Candidate
Simone Moino
matricola: s263114

Academic year 2020-2021

Abstract

The worldwide growing attention to reduce the environmental impact of civil aviation in the next future is clearly visible. At the same time, the goal of achieving high flight speeds is becoming ever more important. During the first parts of the design process, when a quick response to each design modification is required, it is important to have simple and reliable tools to estimate the performances of such vehicles. The aim of the thesis is the development of methodologies and tools for the characterization of propulsive performance of high-speed aircraft in conceptual design. The results of this work allow the evaluation of basic performances for different hypersonic air-breathing propulsive systems architecture and the upgrade of the mathematical models implemented in *ASTRID-H* tool, a conceptual design tool currently under development by Politecnico di Torino. The first part of the research activity carried out for this project have been focusing on the analysis of currently existing engines models for propulsion performance characterization and adequate for conceptual design. Then, thermodynamic models used for subsonic and supersonic engines are implemented and validated with vehicles data, found in literature. Hypersonic engine models are finally designed. Study is made on STRATOFLY MR3 vehicle concept allows 300 passengers to move between places located at the antipodes in few hours, reaching Mach 8 cruise speed, using Liquid Hydrogen as propellant, avoiding the emission of CO_2. This aircraft is based on LAPCAT MR2.4 project and it integrates two combined thermodynamic cycle: Air Turbo Rocket (ATR) is a rocket-based air-breathing engine which are responsible to propel the aircraft from take-off till high-supersonic cruise of Mach 4; after that, vehicle thrust is provided by Dual-Mode Ramjet (DMR), an air-breathing engine that can work in a ramjet configuration (subsonic combustion) or in scramjet one (supersonic combustion). Different models of the two engines are built and analysed, starting from the classic thermodynamic cycle. Finally, Graphical User Interface is implemented, allowing interactive use of propulsive models by a possible user, who does not necessarily have to know the detailed implementation of programmes.

Ringraziamenti

Un sentito grazie a tutte le persone che mi hanno permesso di arrivare fin qui e di portare a termine questo lavoro di tesi.
Ringrazio la Professoressa Nicole Viola, la Dottoressa Roberta Fusaro e il Dottor Davide Ferretto, che mi hanno seguito con grande disponibilità in questi mesi di lavoro, permettendomi di entrare in contatto con il mondo della ricerca.
Ringrazio mamma, papà e Sara, per gli insegnamenti e per l'immmenso supporto datomi in questi anni di studio; senza di loro non avrei mai potuto sostenere questo percorso.
Ringrazio tutti gli amici che mi hanno sostenuto in questi anni, sia il gruppo di più vecchia data della montagna, sia i colleghi dell'università Luca, Davide, Alessandro, Gabriele, Greta e Luca.
Ringrazio, infine, tutti i famigliari e le persone che mi sono state vicine e che mi hanno accompagnato in questi anni.

Grazie infinite a tutti voi.

Contents

List of Tables

List of Figures

Chapter 1

Introduction

[22, 23] Nowadays, one of the main objectives of civil aviation is to reach a certain location in the shortest possible time. This necessity comes from the increasingly close links between countries and companies, even if they are far apart. High-speed aircraft are therefore becoming a viable solution for this: in addition to supersonic flight, hypersonic aircraft will be more important for the commercial transport.
Research in the hypersonic field is very active; it is of fundamental importance the development of a project that can guarantee the hypersonic cruise, respecting economy, safety and environmental impact in terms of emitted noise and greenhouse gasses.
Environmental sustainability is one the main goal of high-speed vehicles development. Liquid Hydrogen plays a key role in hypersonic civil aviation, propellant which seems to be the perfect candidate to substitute hydrocarbon fuel; in fact, LH2 higher energy content reflects directly into the possibility of increasing the flight speed. On the other hand, exploitation of Liquid Hydrogen avoids CO_2 and reduces NO_x emissions, with benefits for environment.
The innovative projects require new studies, starting with the preliminary design phases. For the first steps, a suitable development method is a multi-disciplinary integrated aircraft design approach, which considers the vehicle as the integration of airframe, propulsion and its various subsystems. A conceptual design analysis is of fundamental importance, because it allows an initial dimensioning of the main characteristics of the aircraft; particularly during the early stages of the project, this preliminary analysis allows to have sizing estimation of the various systems, so that they do not have to be modified in the later steps, when changes would cost more in terms of money and time.
In this preliminary design phase, estimation of propulsive performance is of fundamental importance, because it determines the choice of a pre-existing engine or the need to create a new one for the aircraft under consideration. This phase is useful not only for hypersonic flight, but also for classic subsonic and supersonic aircraft. At present, there is no tool that can be used during conceptual design analysis to

obtain initial evaluation of performance of the propulsion system.
ASTRID (Aircraft on-board Systems sizing and TRade-off analysis in Initial Design) and ASTRID-H (Aircraft on-board Systems sizing and TRade-off analysis in Initial Design of High Speed Vehicles), tools developed by research group of Politecnico di Torino, allow conceptual design analysis for subsonic, supersonic and hypersonic civil transport aircraft. They are developed to support the entire methodology of conceptual and preliminary design of civil transportation vehicles and their related subsystems; however, within these programmes there is no part dedicated to engine performance study, the characteristics of which must be known by user.
The aim of thesis work is to develop a software that can help students, engineers and researchers to obtain engine performance during the conceptual design approach. This tool will require some input data, regarding engine characteristic, dimension and propellant, that user has to enter before analysis. Thanks to this work thrust, specific thrust and thrust specific fuel consumption can be evaluated for a specific engine, which can be useful in vehicle conceptual design to size aircraft airframe and components.
For these purpose, engine models based on thermodynamic cycles have to be developed and analysed, so that performances can be obtained. For subsonic and supersonic engine, analysis and design of tool won't be a problem, due to the large number of thermodynamic models already present in literature. On the other hands, data of hypersonic vehicle are difficult to obtain and found; this is due to the high level of difficulty in calculating unusual engine parameters that cannot be compared with more common and classic ones (for example, the end-of-combustion temperature is one of the most complicated to extrapolate). This problem means that the design of hypersonic models is based on thermodynamic cycles of subsonic and supersonic flight, whose models will be modified ad-hoc to obtain new suitable ones for higher flight regimes.

Chapter 2

Basic Models Development

The aim of this work is the development of methodologies and tools for the characterization of propulsive performance of high-speed aircraft in conceptual design. The results of this thesis allow the evaluation of basic performances for different hypersonic air-breathing propulsive systems architecture and the upgrade of the mathematical models implemented in ASTRID-H tool, a conceptual design tool currently under development by Politecnico di Torino. The first part of the research activity carried out for this project have been focusing on the analysis of currently existing engines models for propulsion performance characterization and adequate for conceptual design. Then, implementation on Matlab of thermodynamic models used for subsonic and supersonic engines and their validation with vehicle data, found in literature. Then, analysis and modification on these initial templates has been done to reach the best results for the studied vehicles category.

2.1 Atmospehere Model

Reference [10] is used for atmosphere model. Environmental conditions varying altitude have been necessary to calculate temperature, pressure and density for all the points of thermodynamic cycle. Starting from International Standard Conditions (ISA), magnitudes is found through equations implemented.

- $T_{ISA} = 288.15[K]$

  $p_{ISA} = 101325[Pa]$

  $\rho_{ISA} = 1.225[kg/m^3]$

- $z_s = 11000[m]$

  $T_s = 216.65[K]$

  $p_s = p_{ISA} \cdot (1 - 0.0065 \cdot \frac{z_s}{T_{ISA}})^{5.2561}$

  $\rho_s = \rho_{ISA} \cdot (1 - 0.0065 \cdot \frac{z_s}{T_{ISA}})^{4.2561}$

- $z_{20} = 20000[m]$

  $T_{20} = 216.655[K]$

  $p_{20} = p_s \cdot e^{-g\frac{z_{20}-z_s}{R \cdot T_s}}$

  $\rho_{20} = \rho_s \cdot e^{-g\frac{z_{20}-z_s}{R \cdot T_s}}$

* If altitude is between $0 < z \leq 11000m$:

  $T_0 = T_{ISA} - 0.0065 \cdot z$

  $p_0 = p_{ISA} \cdot (1 - 0.0065 \cdot \frac{z}{T_{ISA}})^{5.2561}$

  $\rho_0 = \rho_{ISA} \cdot (1 - 0.0065 \cdot \frac{z}{T_{ISA}})^{4.2561}$

* If altitude is between $11000 < z \leq 20000m$:

  $T_0 = T_s$

  $p_0 = p_s \cdot e^{-g\frac{z-z_s}{R \cdot T_s}}$

  $\rho_0 = \rho_s \cdot e^{-g\frac{z-z_s}{R \cdot T_s}}$

* If altitude is between $z > 20000m$:

  $T_0 = T_{20} + 0.001 \cdot (z - z_{20})$

$$p_0 = p_{20} \cdot (1 + 0.001 \cdot \frac{z - z_{20}}{T_{20}})^{\frac{-g}{R \cdot 0.001}}$$

$$\rho_0 = \rho_{20} \cdot (1 + 0.001 \cdot \frac{z - z_{20}}{T_{20}})^{\frac{-g}{R \cdot 0.001} - 1}$$

Where T is for temperature, p is for pressure, ρ is for density, z is for altitude.

Varying altitude between 0 and $30000m$, following results are obtained.

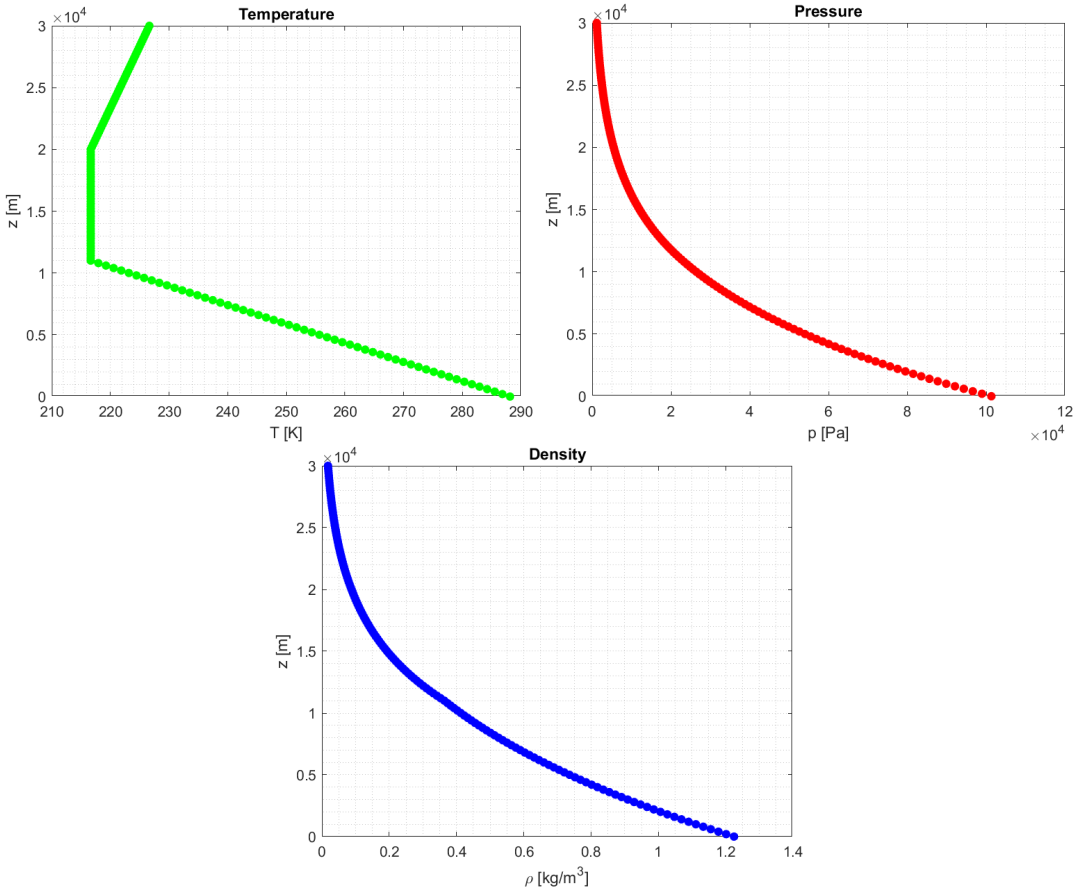

Figure 2.1. Atmosphere model output

2.2 Single-Spool Turbojet

Various references are used for engine model:[1, 2, 5, 7, 8, 11, 9, 12]. The first model analysed is the single-spool turbojet based on Brayton Cycle.
In flowing through the machine, the air undergoes the following processes:

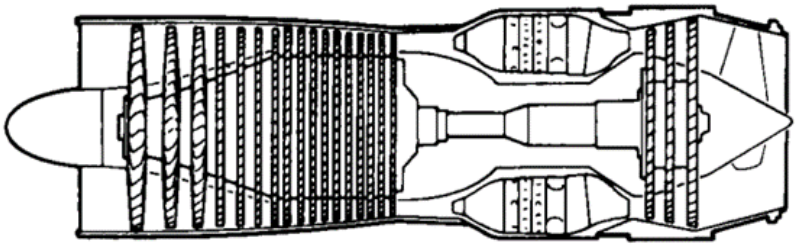

Figure 2.2. Single-spool axial flow turbojet [9]

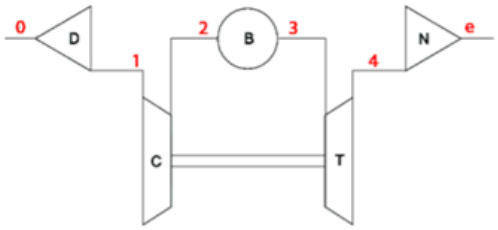

Figure 2.3. Schematic model of a single-spool turbojet [7]

- 0 – 1: From far upstream, where the velocity of the air relative to the engine is the flight velocity, the air is brought to the intake. The air velocity is decreased as the air is carried to the compressor inlet through the inlet diffuser and ducting system.
- 1 – 2: The air is compressed in a single-stage compressor (single stage simplify method).
- 2 – 3: The air is mixed with fuel and burned in the combustion chamber.
- 3 – 4: The air is expanded through a single-stage turbine.
- 4 – e: The air is accelerated and exhausted through the exhaust nozzle.

This cycle is also implemented with afterburner, thanks to the air may or may not be further "heated" by the addition and burning of more fuel after first expansion in turbine, to give engine some extra thrust.

2.2.1 Thermodynamic Cycle

In this Section, the mathematical model describing a single spool turbojet is reported and analysed to evaluate the possibility to implement it in a conceptual

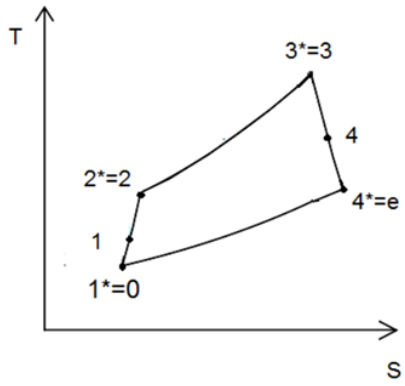

Figure 2.4. Thermodynamic cycle of a single-spool turbojet [5]

design stage.
Evaluating total temperature and pressure after every station, it is possible to calculate outflow rate and engine performances.

- **Intake**
  In each point of the flight profile, the atmospheric model can be used to evaluate the temperature, pressure and density in each specific atmospheric condition; then, known Mach number, total magnitudes of air are calculated.

$$T_0^0 = T_0 \cdot (1 + \frac{\gamma - 1}{2} \cdot M_0^2) \tag{2.1}$$

$$p_0^0 = p_0 \cdot (1 + \frac{\gamma - 1}{2} \cdot M_0^2)^{\frac{\gamma}{\gamma - 1}} \tag{2.2}$$

  Where apex *0* represents total magnitude, γ is the air specific heat ratio and M_0 is the flight Mach number. Then, assuming pneumatic intake efficiency ε_d, corresponding total pressure and temperature are found.

$$T_1^0 = T_0^0 \tag{2.3}$$

$$p_1^0 = \varepsilon_d \cdot p_0^0 \tag{2.4}$$

- **Compressor**
  The second component of the cycle id the compressor, which is responsible of an increase of the stagnation pressure and temperature. Since the overall pressure ratio *OPR* (that in this configuration is equal to single stage compressor

pressure ratio) is specified, it is possible to determine the outlet total pressure and the outlet total temperature, knowing the adiabatic compressor efficiency η_c.

$$T_2^0 = T_1^0 \cdot [1 + \frac{1}{\eta_c} \cdot (OPR^{\frac{\gamma-1}{\gamma}} - 1)] \tag{2.5}$$

$$p_2^0 = OPR \cdot p_1^0 \tag{2.6}$$

- **Combustor**
  In the combustion chamber, thanks to addition of fuel flow and high temperature mixture reaction, flow energy is increased. Temperature after combustion is, generally, one of the known engine parameters; for turbojet, it is called Turbine Inlet Temperature TIT.

$$T_3^0 = TIT \tag{2.7}$$

  Specifying burner outlet temperature T_3^0, it is possible to determine the fuel-air ratio $f = \frac{\dot{m}_b}{\dot{m}_0}$ from balance equation energy of combustor, and fuel flow to.

$$\eta_b \cdot \dot{m}_b \cdot H_i = (\dot{m}_0 + \dot{m}_b) \cdot c_p' \cdot (T_3^0 - T_2^0) \tag{2.8}$$

$$f = \frac{c_p' \cdot (T_3^0 - T_2^0)}{\eta_b \cdot H_i - c_p' \cdot (T_3^0 - T_2^0)} \tag{2.9}$$

  Where $\dot{m}_0$ is air mass flow rate, $\dot{m}_b$ is fuel mass flow rate, η_b is adiabatic burner efficiency, H_i is heat of reaction and c_p' is combusted gases specific heat.
  In other cases, f is known, or it can be supposed (equal to stoichiometric value f_{st}, for example), and temperature after combustion must be calculated. Known pneumatic burner losses ε_b, pressure after combustion is calculated.

$$p_3^0 = \epsilon_b \cdot p_2^0 \tag{2.10}$$

- **Turbine**
  The turbine, moved by the hot gases coming from the combustion, supplies the power required by the compressor. Turbine is the first component where expansion takes place, so it causes total temperature and pressure decrease depending on expansion turbine ratio. Parameters are calculated from balance equation of power between compressor and turbine, knowing mechanic and adiabatic efficiency.

$$T_4^0 = T_3^0 - \frac{c_p}{c_p'} \cdot \frac{1}{\eta_{mt} \cdot \eta_{mc}} \cdot \frac{T_2^0 - T_1^0}{1+f} \tag{2.11}$$

$$p_4^0 = \frac{p_3^0}{\beta_t} \tag{2.12}$$

Where η_{mc} is mechanic compressor efficiency, η_{mt} is mechanic turbine efficiency, β_t is expansion turbine ratio.

- **Nozzle**
  Exhaust nozzle is simply considered as a duct in which the flow accelerates. Exit pressure and temperature can be estimated as follows:

$$p_{cr} = \frac{p_4^0}{\frac{\gamma'+1}{2}^{\frac{\gamma'+1}{\gamma'}}} \tag{2.13}$$

If calm air pressure p_0 is bigger than critic pressure p_{cr},

$$p_e = p_0 \tag{2.14}$$

$$M_e = \sqrt{\frac{2}{\gamma'-1} \cdot \left[\left(\frac{p_4^0}{p_e}\right)^{\frac{\gamma'-1}{\gamma'}} - 1\right]} \tag{2.15}$$

Where γ' is combusted gas specific heat ratio and pedix e is for exit value. Else,

$$p_e = p_{cr} \tag{2.16}$$

$$M_e = 1 \tag{2.17}$$

Temperature and density can be obtained thanks to exit Mach number and ideal gas law,

$$T_e = \frac{T_4^0}{1 + \frac{\gamma'-1}{2} \cdot M_e^2} \tag{2.18}$$

$$\rho_e = \frac{p_e}{R' \cdot T_e} \tag{2.19}$$

Knowing exit temperature, outflow speed w_e can be calculated,

$$w_e = M_e\sqrt{(\gamma' \cdot R' \cdot T_e)} \tag{2.20}$$

If nozzle geometry isn't known, exit area can be calculated for the design point and the value obtained shall be used for the entire process. Nozzle outflow mass is equal to the sum of propellant mass flow rate and inlet mass flow rate (in ideal condition, where mass flow losses aren't considered), so,

$$A_e = \frac{\dot{m}_0 + \dot{m}_b}{\rho_e \cdot w_e} \tag{2.21}$$

- **Afterburner**
  In case an afterburner is present, it can easily added to the mathematical model as follows. In the afterburner, an additional amount of fuel is injected into a combustor in the jet pipe behind the turbine, "reheating" the exhaust gas. Consequently, the temperature rises before reaching the nozzle area and resulting in a thrust increase. Knowing afterburner exit temperature and afterburner propellant mass flow, it is possible to obtained exit nozzle value like in Equations 2.13 - 2.24. From critic pressure value, exit Mach value is calculated. Then, exit temperature, pressure and speed are obtained:

$$T_{e_{ab}} = \frac{T^0_{e_{ab}}}{1 + \frac{\gamma'-1}{2} \cdot M^2_{e_{ab}}} \tag{2.22}$$

$$\rho_{e_{ab}} = \frac{p_{e_{ab}}}{R' \cdot T_{e_{ab}}} \tag{2.23}$$

$$w_{e_{ab}} = M_{e_{ab}}\sqrt{(\gamma' \cdot R' \cdot T_{e_{ab}})} \tag{2.24}$$

  Where pedix ab is for afterburner.
  As in Equation 2.21, if afterburner-nozzle geometry isn't known, it can be calculated for the design point:

$$A_{e_{ab}} = \frac{\dot{m}_0 + \dot{m}_b + \dot{m}_{ab}}{\rho_{e_{ab}} \cdot w_{e_{ab}}} \tag{2.25}$$

2.2.2 Input Data

This part concerns necessary data to evaluate engine performances. Inputs can be inserted by user if engine is known, they can be evaluated through statistical analysis or they can be suggested by software. During turbojet model development J85, developed by *General Electric*, is used to validate model working. In the following graph, input data are reported.

COEFFICIENT	VALUE
Air and Fuel Data	
Universal gas constant, R	*287 [J/(kg*K)]*
Combusted gases constant, R'	*293 [J/(kg*K)]*
Air specific heat, c_p	*1004 [J/(kg*K)]*
Combusted gases specific heat, c'_p	*1184 [J/(kg*K)]*
Air specific heat ratio, γ	*1.375*
Combusted gases specific heat ratio, γ'	*1.3*
Heat of reaction, H_i	*43.26 [MJ/kg]*
Engine Data	
Intake	
Mass flow rate, $\dot{m}$	*19.9 [kg/s]*
Pneumatic intake efficiency, ε_d	*0.98*
Compressor	
Overall Pressure Ratio, OPR	*8.3*
Mechanic compressor efficiency, η_{mc}	*1*
Adiabatic compressor efficiency, η_c	*0.822*
Combustor	
Turbine Inlet Temperature, TIT	*1260 [K]*
Pneumatic combustor efficiency, ε_b	*1*
Combustion efficiency, η_b	*0.982*
Turbine	
Mechanic turbine efficiency, η_{mt}	*0.95*
Adiabatic turbine efficiency, η_t	*0.822*
Afterburner	
Afterburner exit temperature, $T_{e_{ab}}$	*1700 [K]*
Afterburner propellant mass flow, $\dot{m}_{ab}$	*0.417 [kg/s]*
Pneumatic afterburner efficiency, ε_{ab}	*1*
Afterburning efficiency, η_{ab}	*0.9*

Table 2.1. Turbojet input data

Turbojet cycle needs also the atmospheric model presented before. It evaluates performances at fixed point, altitude and Mach number decided by user, or it gives results varying altitude and Mach number between established values. During all phases of thermodynamic cycle, two types of flow are considered, simple air flow and combusted gases flow, with the values reported in Table 2.1; specific heat ratio of air and combusted gases are supposed constant during all process. Stations numbering used is the one illustrated in Figure 2.3 and Figure 2.4.

2.2.3 Propulsive Performance Characterization

Once the engine cycle parameters are estimated, main engine performance can be evaluated in different flight conditions.

- **Thrust**

  Available thrust in without afterburner can be estimated using the following equation:

$$T = \dot{m}_0 \cdot [(1 + f) \cdot w_e - u] + A_e \cdot (p_e - p_0) \tag{2.26}$$

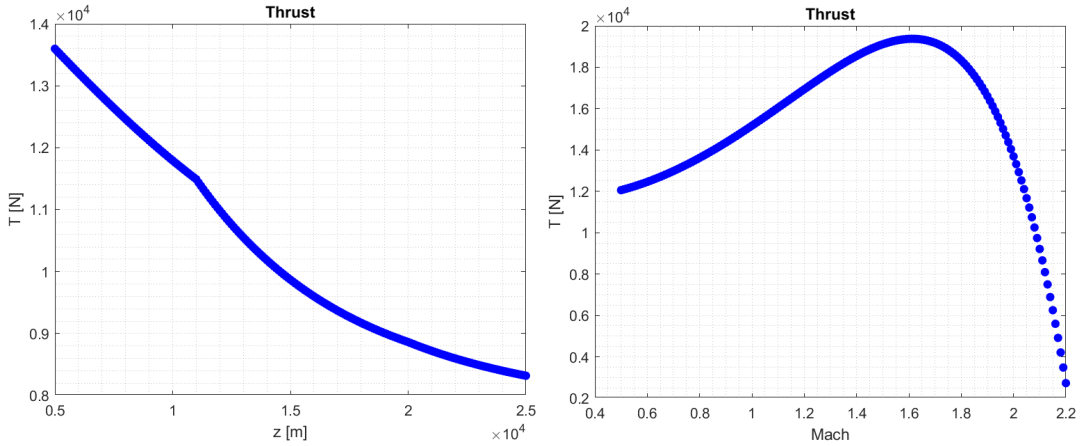

Figure 2.5. General Electric J85 thrust varying altitude and Mach

Figure 2.5 shows thrust variation for two parameters that change during flight. Static temperature, pressure and density change with altitude, while air mass flow changes with Mach, as previous subsection equations show; therefore, change in height and speed causes thrust shift. Altitude and Mach number are firstly represented separately to evaluate in the best way basic model responses. For the final ATR and DMR implementations, they will be put together to give a better idea of thrust variation during the whole mission profile. 'Results obtained are in line with what was found in literature: *J85 General Electric* nominal thrust is equal to *16 kN* without afterburner and *22 kN* with afterbuner switched-on[1].'
In Figure 2.6 thrust variation with afterburner switch-on is compared to the previous case. The addition of heat permits reachness of greatest altitude and Mach number, increasing, on the other hand, fuel consumption.

[1]General Electric J85, *Wikipedia*

$$T_{ab} = \dot{m}_0 \cdot [(1+f) \cdot w_{e_{ab}} - u] + A_{e_{ab}} \cdot (p_{e_{ab}} - p_0) \tag{2.27}$$

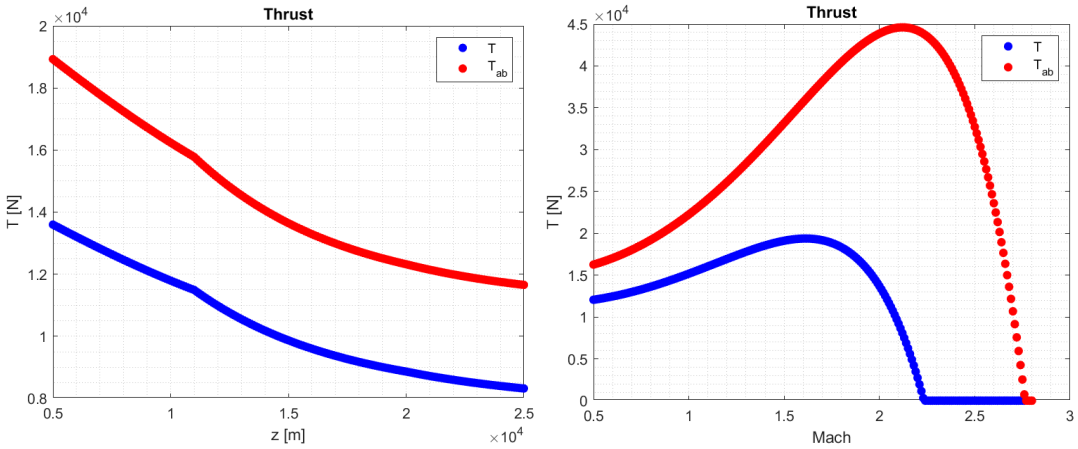

Figure 2.6. General Electric J85 thrust with and without afterburning phase

- **Specific Thrust**

  Specific thrust evaluation can be useful to compare engine of different dimension and performances; as equation 2.28 shows, this magnitude is proportional to thrust.

$$I_a = \frac{T}{\dot{m}_0} \tag{2.28}$$

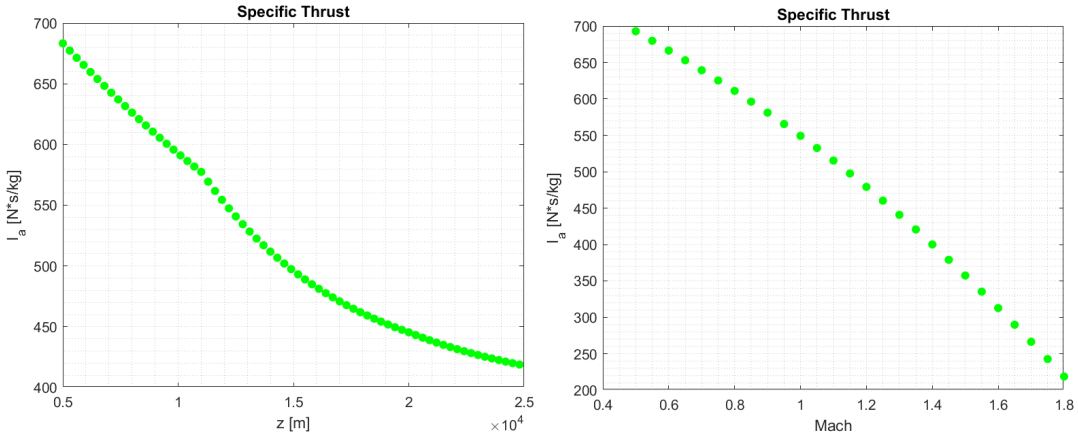

Figure 2.7. General Electric J85 specific thrust varying altitude and Mach

- **Thrust Specific Fuel Consumption**

  Thrust specific fuel consumption or *TSFC* represents fuel utilised by engine to give certain thrust; it gives an idea of engine consumption and, as shown in equations 2.40 and 2.30, it is proportional to thrust.

$$I_{sp} = \frac{\dot{m}_b}{T} \tag{2.29}$$

$$I_{sp_{ab}} = \frac{\dot{m}_b + \dot{m}_{ab}}{T_{ab}} \tag{2.30}$$

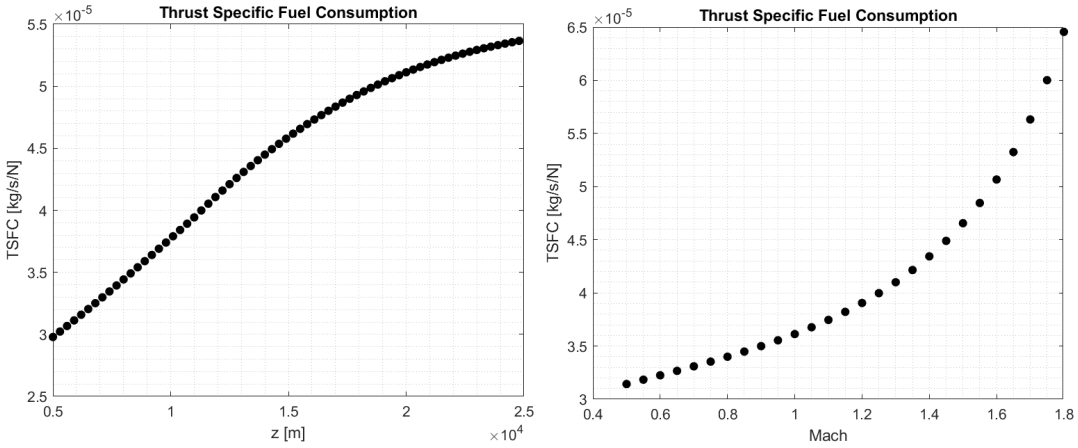

Figure 2.8. General Electric J85 TSFC varying altitude and Mach

2.3 Ramjet

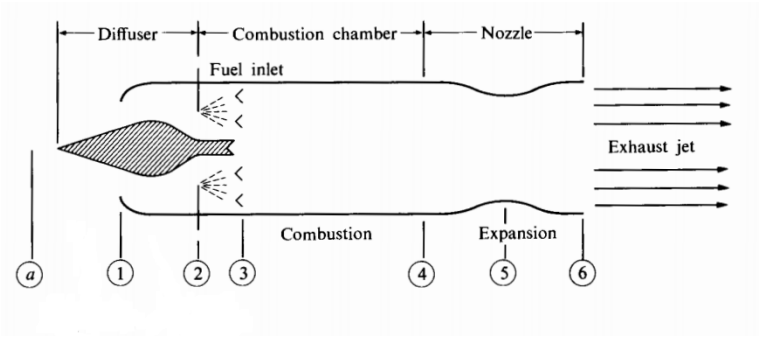

Figure 2.9. Ramjet [9]

Various references are used for engine model:[1, 4, 5, 7, 9]. In general, any air-breathing vehicle must send a certain air quantity to combustion chamber, so that engine can guarantee thrust for acceleration. For classic turbojet and turbofan engine, this aim is made by intake and compressor (moved by turbine); turbine inlet temperature is the limiting factor for these type of engine in achieving high specific thrust. "At flight speeds exceeding approximately Mach 3, the compressor is no longer required to achieve sufficient cycle-pressure ratio, and the ramjet becomes the propulsion cycle of choice. As flight speed is still further increased, the supersonic combustion ramjet (scramjet) cycle becomes the engine cycle of choice because it does not require excessive speed reduction of the high-enthalpy mainstream airflow."[2]
Model developed in this chapter will be also utilized for the hypersonic flight; this approximation can be considered good enough if results are similar to expected values, keeping in mind that this type of programm will be used for the preliminary conceptual design process.

Deleting compressor and turbine stages from turbojet engine, ramjet can be considered the simplest thermodynamic model. In fact, it consists of a diffuser, a combustion chamber and an exhaust nozzle, as shown in Figure 2.10.
As in turbojet case, engine division is the following.

- 0 - 1 $\equiv$ 2: Air flow reaches the diffuser with a certain speed and, passing through the intake, it arrives in the combustion chamber.

[2]E.T. Curran, S.N.B. Murthy, *Scramjet Propulsion*, Volume 189 PROGRESS IN ASTRONAUTICS AND AERONAUTICS

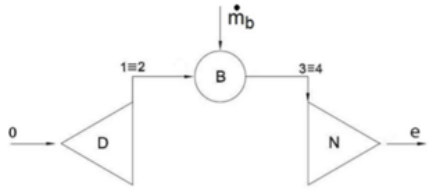

Figure 2.10. Ramjet schematic model [7]

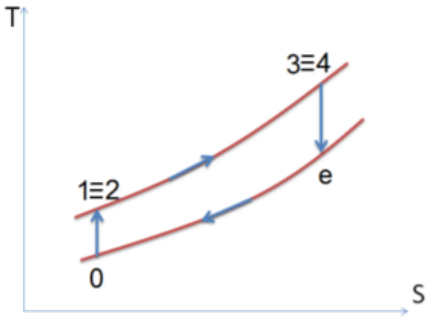

Figure 2.11. Ramjet thermodynamic cycle [7]

- 2 - 3: Process is treated as the same as turbojet combustion: air is mixed with fuel and burned.
- 3 ≡ 4 - e: Air flow is accelerated and exhausted through nozzle.

Thermodynamic cycle represented in Figure 2.11 is the ideal one, so no losses considered. However, during the process, pressure losses and burner efficiency can be inserted.

2.3.1 Thermodynamic Cycle

Thanks to calculation of total temperature and pressure through engine steps, final speed can be found.

- **Intake**
  In this analysis, the diffuser is very simple: pressure losses ε_d consider every kind of dissipation from inlet to combustor and it permits to reach the correct total pressure needed for combustion. In the ideal case, no temperature losses are implemented.

$$T_2^0 = T_1^0 = T_0^0 \tag{2.31}$$

$$p_2^0 = p_1^0 = \varepsilon_d \cdot p_0^0 \tag{2.32}$$

- **Combustor**
  As in turbojet case, from Equation 2.8, f can be found knowing temperature after combustion process.

$$f = \frac{c_p' \cdot (T_3^0 - T_2^0)}{\eta_b \cdot H_i - c_p' \cdot (T_3^0 - T_2^0)} \tag{2.33}$$

  As before, if f is known or conceivable, temperature could be found. Total pressure are taken in count during combustion.

$$p_4^0 = p_3^0 = \varepsilon_b \cdot p_2^0 \tag{2.34}$$

  Where ε_b is burner pneumatic efficiency.

- **Nozzle**
  This first and simplest ramjet treatment considers adaptive nozzle. Exit flow speed is calculated without geometry data, but only knowing exit total temperature and pressure. In the next chapter, a more detailed model, using nozzle area) is implemented for the Dual-Mode Ramjet.

$$T_e^0 = T_4^0 \tag{2.35}$$

$$p_e^0 = \varepsilon_n \cdot p_4^0 \tag{2.36}$$

  Where ε_n is nozzle pneumatic efficiency.

$$w_e = \sqrt{2 \cdot c_p' \cdot T_e^0 \cdot \left[1 - \left(\frac{p_0}{p_e^0}\right)^{\frac{\gamma'-1}{\gamma'}}\right]} \tag{2.37}$$

2.3.2 Input Data

First difficulty for ramjet model is finding data; reason is that almost all this engine is only theoretical project or they are prototype. So, model evaluation is done around supposed data and not on a specific engine.
Results of this model are calculated for different Mach number and altitude, finding graphs as in turbojet case.

COEFFICIENT	VALUE
Air and Fuel Data	
Universal gas constant, R	*287 [J/(kg*K)]*
Combusted gases constant, R'	*293 [J/(kg*K)]*
Air specific heat, c_p	*1004 [J/(kg*K)]*
Combusted gases specific heat, c'_p	*1184 [J/(kg*K)]*
Air specific heat ratio, γ	*1.4*
Combusted gases specific heat ratio, γ'	*1.36*
Heat of reaction, H_i	*45 [MJ/kg]*
Engine Data	
Temperature after combustion, T_3^0	*2000 [K]*
Diffuser area, A_0	*37.7 [m^2]*
Pneumatic intake efficiency, ε_d	*0.95*
Pneumatic combustor efficiency, ε_b	*1*
Pneumatic nozzle efficiency, ε_n	*1*
Combustion efficiency, η_b	*0.9*

Table 2.2. Ramjet input data

2.3.3 Propulsive Performance Characterization

From thermodynamic cycle presented before, thrust, specific thrust and thrust specific fuel consumption can be found.

- **Thrust**

  For an adaptive nozzle, thrust does not take in count of second contribute as in Equation 2.26.

$$T = (\dot{m}_0 + \dot{m}_b) \cdot w_e - \dot{m}_0 \cdot u \tag{2.38}$$

  Fixing temperature after combustion, results obtained are shown in Figure 2.12.

  Thrust decrease gradually with altitude, due to air pressure and density reduction. On the other hand, it's possible to see that it reaches the maximum value around $M = 3 \div 3.5$. Thrust trend is in line with literature data; in fact, for Mach number greater than 5 ramjet will be unuseful (such as the lowest flight speed) and scramjet engine with supersonic combustion will be necessary.
  A possibility to develop ramjet engine that works for Mach number higher than 5, like a scrmajet, is temperature after combustion increase. From Figure 2.13

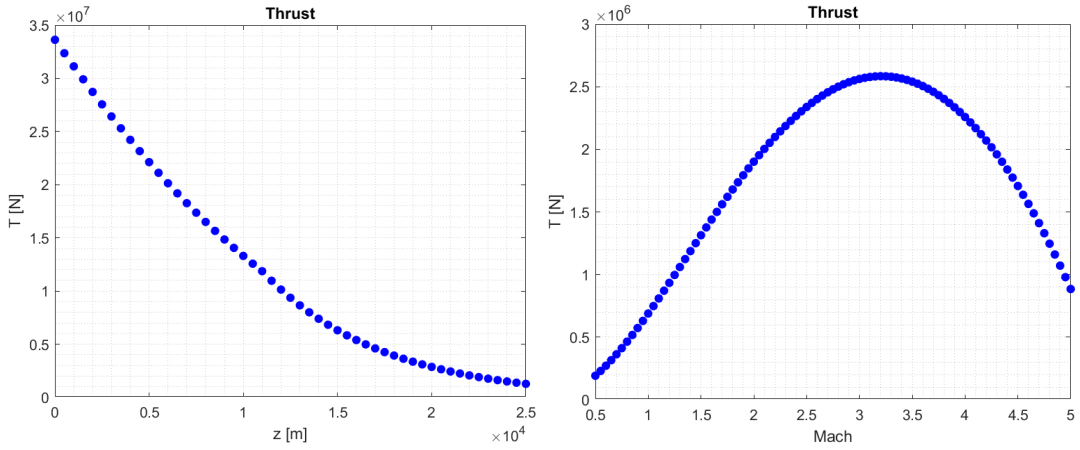

Figure 2.12. Ramjet thrust varying altitude and Mach

this effect can be seen, observing maximum thrust translation to greater Mach number.

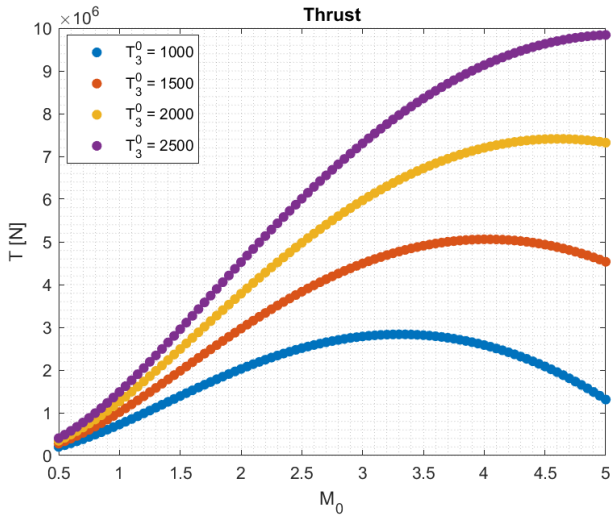

Figure 2.13. Ramjet thrust varying Mach and temperature after combustion

- **Specific Thrust**

Equation 2.28 can be derived as:

$$I_a = \frac{T}{\dot{m}_0} = (1+f)\cdot w_e - u \tag{2.39}$$

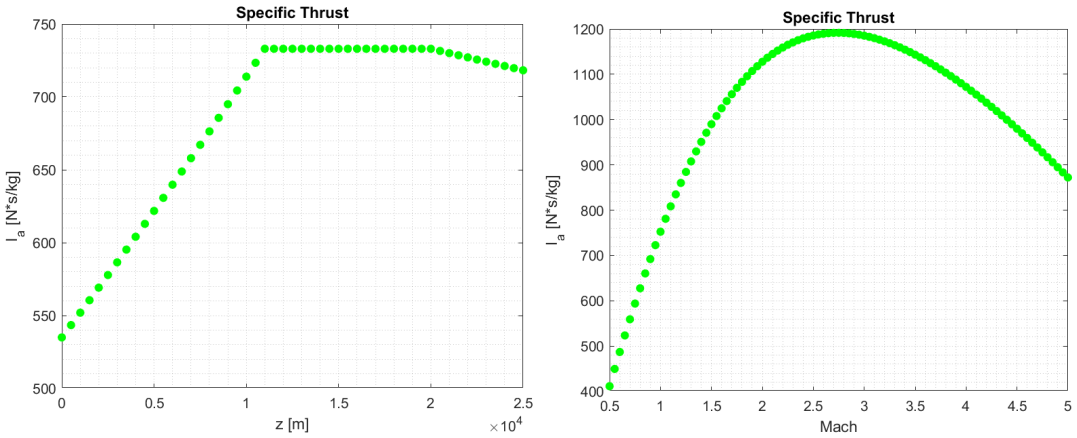

Figure 2.14. Ramjet specific thrust varying altitude and Mach

- **Thrust Specific Fuel Consumption**

$$I_{sp} = \frac{\dot{m}_b}{T} \tag{2.40}$$

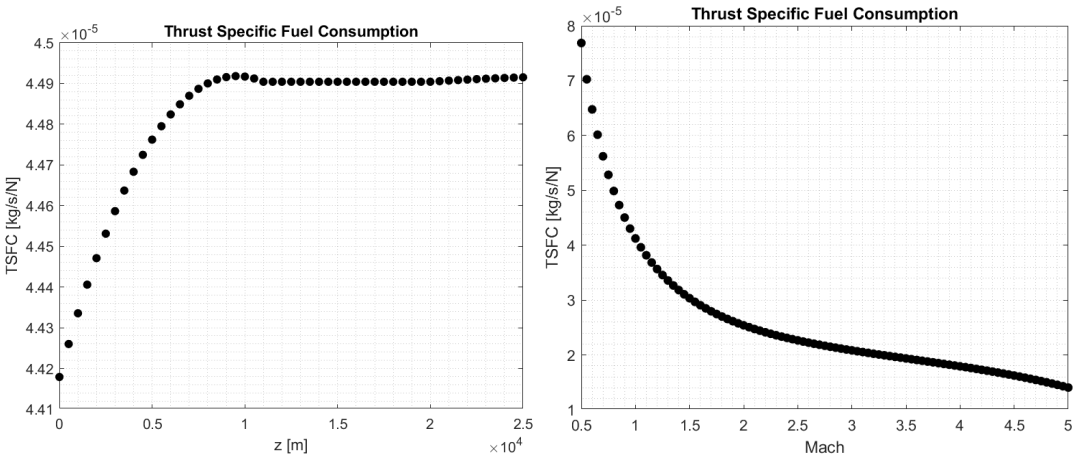

Figure 2.15. Ramjet TSFC varying altitude and Mach

For supersonic flight speed *TSFC* reaches lower values, more acceptable than for $M_0 < 1.5$. For the greatest Mach numbers, Figure 2.15 isn't useful, because of ramjet inefficiency.

2.4 Twin-Spool Turbojet

Various references are used for engine model: [1, 2, 7, 8, 9, 11, 12]. This and the next section present two other type of engine, used for subsonic and supersonic flight, which won't be useful for the hypersonic propulsive development; however, these models can be utilised in ASTRID for a more complex and completed analysis from the propulsion point of view.
Twin-spool turbojet example can be *Olympus 593* by *Rolls-Royce/Snecma*; this type of engine can be useful to reach supersonic flight speed. The Olympus 593 was installed on Concorde and it was formed by 2 shaft and an afterburner, that permits supersonic Mach reach.

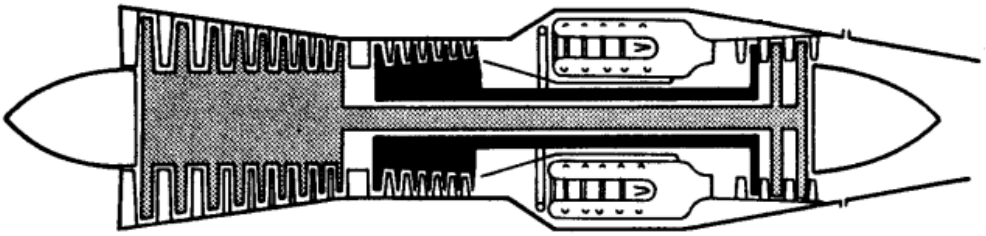

Figure 2.16. Olympus 593 [6]

Thermodynamic cycle is quite similar to single-spool turbojet one represented in Figure 2.4; adding two intermediate points in compression and expansion phases, low-pressure shaft and high-pressure shaft will be featured.

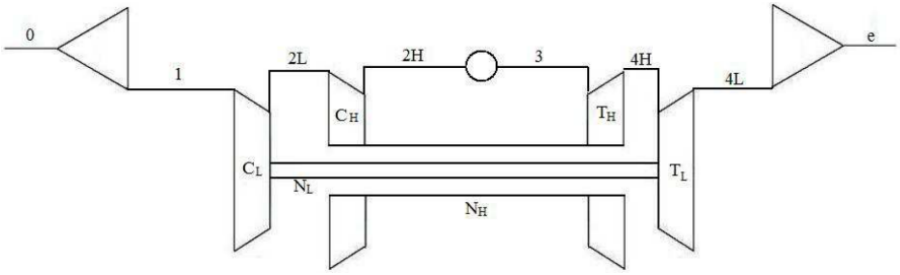

Figure 2.17. Schematic model of a twin-spool turbojet [5]

Engine can be divided in the following sections:

- 0 – 1: Inlet duct.
- 1 - 2L: Low-pressure compressor.
- 2L - 2H: High-pressure compressor.

- 2H – 3: Combustion chamber.
- 3 – 4H: High-pressure turbine, connected to high-pressure compressor by high-pressure shaft (N_H).
- 4H – 4L: Low-pressure turbine, connected to low-pressure compressor by low-pressure shaft (N_L).
- 4L – e: Exhaust nozzle.

2.4.1 Thermodynamic Cycle

- **Intake**
  After total temperature and pressure calculation (Equations 2.1 and 2.2), exit intake conditions can be evaluated in the same way of single-spool turbojet.

$$T_1^0 = T_0^0 \tag{2.41}$$

$$p_1^0 = \varepsilon_d \cdot p_0^0 \tag{2.42}$$

  Where ε_d is pneumatic intake efficiency.

- **Low-pressure compressor**
  Differently from single-spool turbojet, bi-shaft engine have two different compression phases: first one increases pressure and temperature proportionally to the lowest β_{cL} (low compressor ratio).

$$T_{2L}^0 = T_1^0 \cdot [1 + \frac{1}{\eta_{cL}} \cdot (\beta_{cL}^{\frac{\gamma-1}{\gamma}} - 1)] \tag{2.43}$$

$$p_{2L}^0 = \beta_{cL} \cdot p_1^0 \tag{2.44}$$

  Where η_{cL} is the adiabatic low-pressure compressor efficiency and β_{cL} is the low-pressure compressor ratio.

- **High-pressure compressor**
  After first compression, the second one takes air to correct values necessary for combustion.

$$T_{2H}^0 = T_{2L}^0 \cdot [1 + \frac{1}{\eta_{cH}} \cdot (\beta_{cH}^{\frac{\gamma-1}{\gamma}} - 1)] \tag{2.45}$$

$$p_{2H}^0 = \beta_{cH} \cdot p_{2L}^0 \tag{2.46}$$

Where η_{cH} is the adiabatic high-pressure compressor efficiency and β_{cH} is the high-pressure compression ratio.

- **Combustor**
  Combustion process is the same of precedent one. From Equation 2.8, f is calculated as in Equation 2.9.

$$f = \frac{c'_p \cdot (T_3^0 - T_{2H}^0)}{\eta_b \cdot H_i - c'_p \cdot (T_3^0 - T_{2H}^0)} \tag{2.47}$$

  Total pressure is obtained like in Equation 2.10.

- **High-pressure turbine**
  As for compressor cases, expansion takes place in two different group turbine, respectively connected to compressor between corresponding shaft.

$$T_{4H}^0 = T_3^0 - \frac{c_p}{c'_p} \cdot \frac{1}{\eta_{mtH} \cdot \eta_{mcH}} \cdot \frac{T_{2H}^0 - T_{2L}^0}{1+f} \tag{2.48}$$

$$p_{4H}^0 = \frac{p_3^0}{\beta_{tH}} \tag{2.49}$$

  Where η_{mtH} is mechanic high-pressure turbine efficiency, η_{mcH} is mechanic high-pressure compressor efficiency and β_{tH} is expansion high-pressure turbine ratio.

- **Low-pressure turbine**
  In the same way for low-pressure turbine.

$$T_{4L}^0 = T_{4H}^0 - \frac{c_p}{c'_p} \cdot \frac{1}{\eta_{mtL} \cdot \eta_{mcL}} \cdot \frac{T_{2L}^0 - T_1^0}{1+f} \tag{2.50}$$

$$p_{4L}^0 = \frac{p_{4H}^0}{\beta_{tL}} \tag{2.51}$$

  Where η_{mtL} is mechanic high-pressure turbine efficiency, η_{mcL} is mechanic high-pressure compressor efficiency and β_{tL} is expansion high-pressure turbine ratio.

- **Nozzle**
  Exhaust nozzle can be treated in the same way of single-spool turbojet. From Equations 2.13 - 2.19, exit speed can be found.

$$w_e = M_e \sqrt{(\gamma' \cdot R' \cdot T_e)} \tag{2.52}$$

2.4.2 Input Data

COEFFICIENT	VALUE
Air and Fuel Data	
Universal gas constant, R	*287 [J/(kg*K)]*
Combusted gases constant, R'	*293 [J/(kg*K)]*
Air specific heat, c_p	*1004 [J/(kg*K)]*
Combusted gases specific heat, c'_p	*1184 [J/(kg*K)]*
Air specific heat ratio, γ	*1.375*
Combusted gases specific heat ratio, γ'	*1.3*
Heat of reaction, H_i	*43.26 [MJ/kg]*
Engine Data	
Intake	
Mass flow rate, $\dot{m}$	*186 [kg/s]*
Pneumatic intake efficiency, ε_d	*0.98*
Low-Pressure Compressor	
Low Compression Ratio, β_{cL}	*3.237*
Mechanic compressor efficiency, η_{mcL}	*1*
Adiabatic compressor efficiency, η_{cL}	*0.87*
High-Pressure Compressor	
High Compression Ratio, β_{cH}	*4.788*
Mechanic compressor efficiency, η_{mcH}	*1*
Adiabatic compressor efficiency, η_{cH}	*0.87*
Combustor	
Turbine Inlet Temperature, *TIT*	*1012.15 [K]*
Pneumatic combustor efficiency, ε_b	*1*
Combustion efficiency, η_b	*0.98*
High-Pressure Turbine	
Mechanic turbine efficiency, η_{mtH}	*0.95*
Adiabatic turbine efficiency, η_{tH}	*0.93*
Low-Pressure Turbine	
Mechanic turbine efficiency, η_{mtL}	*0.95*
Adiabatic turbine efficiency, η_{tL}	*0.93*

Table 2.3. Twin-spool turbojet input data

Olympus 593 input data are reported in Table 2.3. Even if engine was developed with afterburner, the following treatment won't analyse this function, because it has the same behaviour presented in single-spool turbojet section.

2.4.3 Propulsive Performance Characterization

All results represented in this subsection are quite similar to single-spool turbojet, as expected.

- **Thrust**

$$T = \dot{m}_0 \cdot [(1+f) \cdot w_e - u] + A_e \cdot (p_e - p_0) \tag{2.53}$$

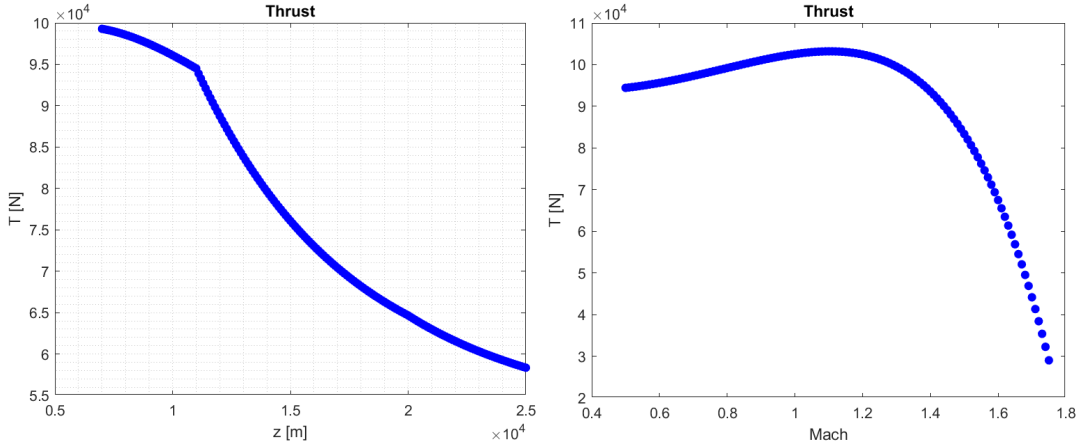

Figure 2.18. Olympus 593 thrust varying altitude and Mach

- **Specific Thrust**

$$I_a = \frac{T}{\dot{m}_0} \tag{2.54}$$

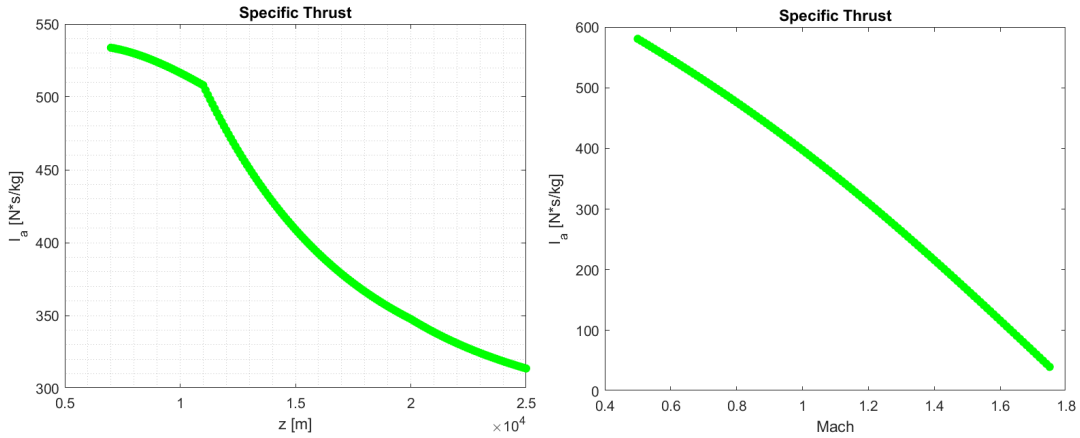

Figure 2.19. Olympus 593 specific thrust varying altitude and Mach

- **Thrust Specific Fuel Consumption**

$$I_{sp} = \frac{\dot{m}_b}{T} \tag{2.55}$$

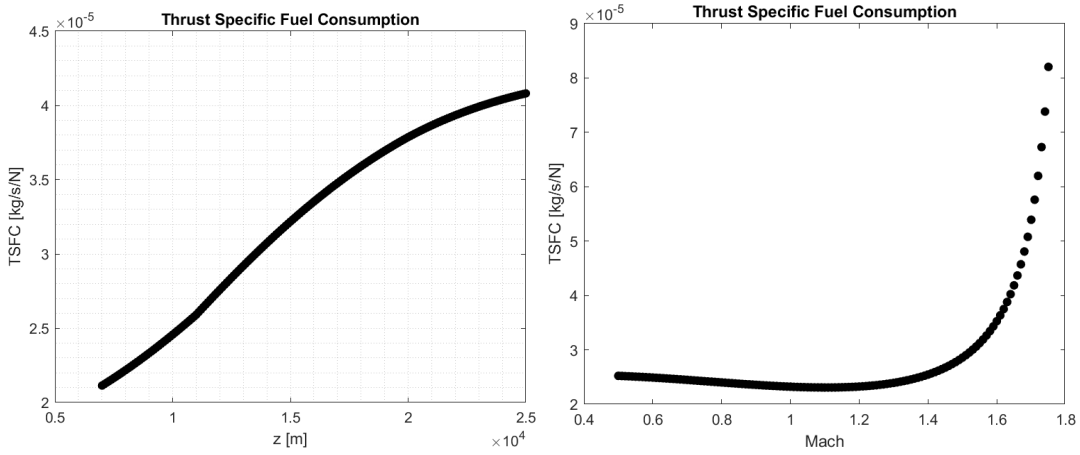

Figure 2.20. Olympus 593 TSFC varying altitude and Mach

2.5 Turbofan

Various references are used for engine model: [1, 2, 5, 7, 8, 9, 12]. "The turbofan engine was originally conceived as a method of improving the propulsion efficiency of the jet engine by reducing the mean jet velocity, particularly for operation at high subsonic speeds. In this type of engine a portion of the total flow bypasses part of the compressor, combustion chamber, turbine and nozzle before being ejected through a separate nozzle" [3]

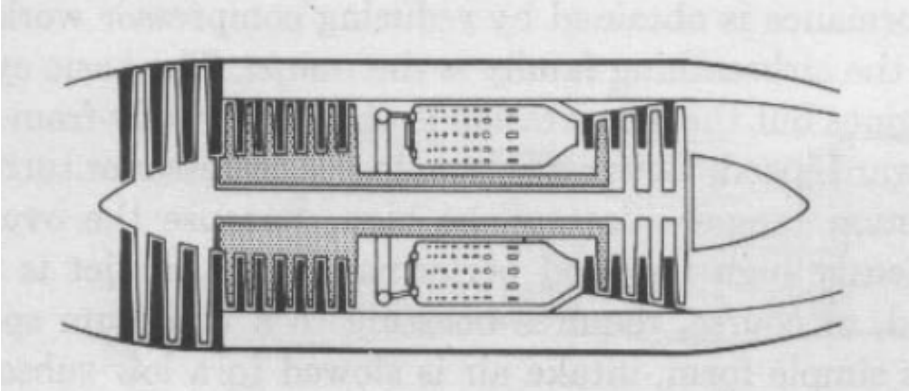

Figure 2.21. Representation of a separated-flow turbofan [9]

The type of turbofan described is called separated-flow turbofan, or high by-pass ratio turbofan, because *BPR* value is often bigger then in mixed-flow configurations, or low by-pass ratio turbofan.

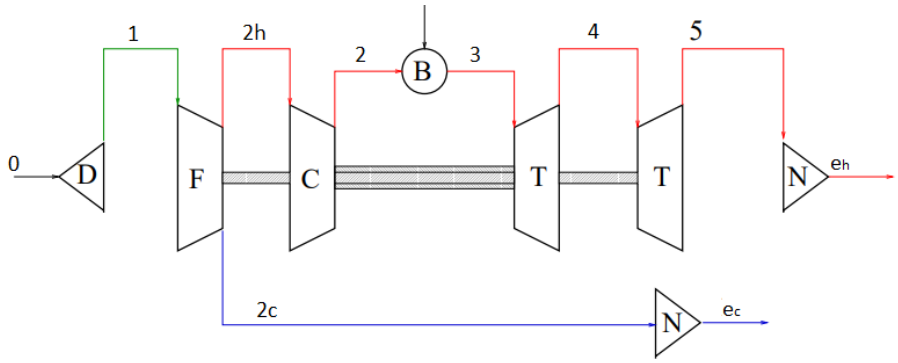

Figure 2.22. Separated-flow turbofan model [5]

As reported in Figure 2.22, engine cycle is divided in the following step:

[3]H. I. H. Saravanamuttoo, G. F. C. Rogers, H. Cohen, *GAS TURBINE THEORY*, PEARSON

- 0 – 1: Inlet duct.
- 1 - 2h: Fan compression ('hot' flow, so combusted part).
- 1 - 2c: Fan compression ('cold' flow, not combusted part).
- 2h - 2: Compressor stages.
- 2 – 3: Combustor.
- 3 – 4: High-pressure turbine stages, connected to compressor.
- 4 – 5: Low-pressure turbine stages, connected to fan.
- 5 – e_h: Exhaust 'hot' flow nozzle.
- 2c – e_c: Exhaust 'cold' flow nozzle.

Turbofan thermodynamic cycle is similar to twin-spool turbojet one.

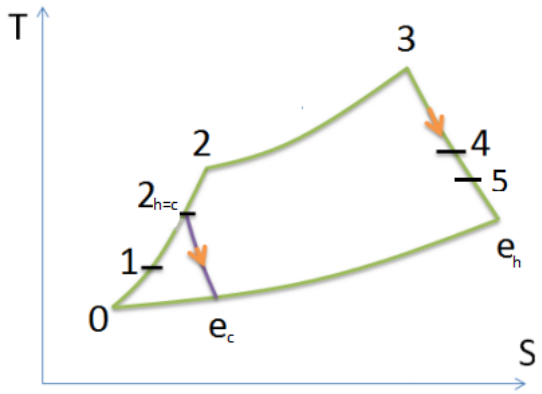

Figure 2.23. Thremodynamic cycle of a separated-flow turbofan [7]

2.5.1 Thermodynamic Cycle

- **Intake**
  After total temperature and pressure calculation (Equations 2.1 and 2.2), exit intake conditions can be evaluated in the same way of single-spool turbojet.

$$T_1^0 = T_0^0 \tag{2.56}$$

$$p_1^0 = \varepsilon_d \cdot p_0^0 \tag{2.57}$$

Where ε_d is the pneumatic intake efficiency.

- **Fan**
  Fan could be treated as the low-pressure compressor of twin-spool turbojet. However, it is characterized by minor compression ratio then turbojet; part of air pressurized by fan isn't sent to combustion chamber, but it passes through the engine and reaches a dedicated 'cold' nozzle (in separated flow turbofan configuration).

$$T_{2c}^0 = T_1^0 \cdot [1 + \frac{1}{\eta_f} \cdot (FPR^{\frac{\gamma-1}{\gamma}} - 1)] \tag{2.58}$$

$$p_{2c}^0 = FPR \cdot p_1^0 \tag{2.59}$$

  Where η_f is the adiabatic fan efficiency and FPR is the fan pressure ratio.

  Fan pressurized 'hot' air directed to burner has the same properties of 'cold' air.

$$T_{2h}^0 = T_{2c}^0 \tag{2.60}$$

$$p_{2h}^0 = p_{2c}^0 \tag{2.61}$$

  Thanks to by-pass ratio it is possible to calculate mass-flow rate sent to distinct engine part.

$$\dot{m}_h = \frac{\dot{m}_0}{1 + BPR} \tag{2.62}$$

$$\dot{m}_c = \dot{m}_0 - \dot{m}_h \tag{2.63}$$

  Where BPR is the by-pass ratio, while subscripts h is for hot and c for cold.

- **Compressor**
  After first compression, the second one takes air to combustion chamber, further increasing temperature and pressure.

$$T_2^0 = T_1^0 \cdot [1 + \frac{1}{\eta_c} \cdot (OPR^{\frac{\gamma-1}{\gamma}} - 1)] \tag{2.64}$$

$$p_2^0 = OPR \cdot p_1^0 \tag{2.65}$$

  Where η_c is the adiabatic compressor efficiency and OPR is the overall pressure ratio, including compressor stages and fan.

- **Combustor**
  Combustion process is the same of precedent ones. From Equation 2.8, f is calculated as in Equation 2.9.

$$f = \frac{c'_p \cdot (T_3^0 - T_2^0)}{\eta_b \cdot H_i - c'_p \cdot (T_3^0 - T_2^0)} \tag{2.66}$$

  However, fuel mass flow rate is calculated differently.

$$\dot{m}_b = \dot{m}_c \cdot f \tag{2.67}$$

  Total pressure is obtained like in Equation 2.10.

- **High-pressure turbine**
  As for compressor cases, expansion takes place in two different group turbine, respectively connected to compressor between corresponding shaft.

$$T_4^0 = T_3^0 - \frac{c_p}{c'_p} \cdot \frac{1}{\eta_{mtH} \cdot \eta_{mc}} \cdot \frac{T_2^0 - T_{2h}^0}{1+f} \tag{2.68}$$

$$p_4^0 = \frac{p_3^0}{\beta_{tH}} \tag{2.69}$$

  Where η_{mtH} is mechanic high-pressure turbine efficiency, η_{mcH} is mechanic high-pressure compressor efficiency and β_{tH} is expansion high-pressure turbine ratio.

- **Low-pressure turbine**
  High-pressure turbine process is utilised for low-pressure turbine.

$$T_5^0 = T_4^0 - \frac{c_p}{c'_p} \cdot \frac{1}{\eta_{mtL} \cdot \eta_{mf}} \cdot \frac{T_{2h}^0 - T_1^0}{1+f} \tag{2.70}$$

$$p_5^0 = \frac{p_4^0}{\beta_{tL}} \tag{2.71}$$

  Where η_{mtL} is mechanic high-pressure turbine efficiency, η_{mcL} is mechanic high-pressure compressor efficiency and β_{tL} is expansion high-pressure turbine ratio.

- **Nozzle**
  Exhaust 'hot' nozzle can be treated in the same way of single-spool turbojet. From Equations 2.13 - 2.19, exit 'hot' flow speed w_{e_c} can be found.

$$w_{e_c} = M_{e_c}\sqrt{(\gamma' \cdot R' \cdot T_{e_c})} \tag{2.72}$$

  'Cold' nozzle is treated as adapted instead, so $p_{e_c} = p_0$ different contribution in thrust equation will be considered. Exit 'cold' flow speed w_{e_f} is found in the following way.

$$w_{e_f} = \sqrt{2 \cdot c_p \cdot T^0_{2c} \cdot \eta_{n_c} \cdot \left[1 - \left(\frac{p_0}{p^0_{2f}}\right)^{\frac{\gamma-1}{\gamma}}\right]} \tag{2.73}$$

2.5.2 Input Data

Separeted-flow turbofan model validation is done studying *JT9D* by *Pratt and Whitney*, one of the first turbofan built. Trying to simplify model, single compressor group is implemented considering global OPR, so that a larger numbers of engine can be analysed using one software.

COEFFICIENT	VALUE
Air and Fuel Data	
Universal gas constant, R	*287 [J/(kg*K)]*
Combusted gases constant, R'	*293 [J/(kg*K)]*
Air specific heat, c_p	*1004 [J/(kg*K)]*
Combusted gases specific heat, c'_p	*1184 [J/(kg*K)]*
Air specific heat ratio, γ	*1.375*
Combusted gases specific heat ratio, γ'	*1.3*
Heat of reaction, H_i	*43.26 [MJ/kg]*
Engine Data	
Intake	
Mass flow rate, $\dot{m}$	*684 [kg/s]*
Pneumatic intake efficiency, ε_d	*0.98*
Fan	
Fan Pressure Ratio, *FPR*	*1.6*
By-Pass Ratio, *BPR*	*5.17*
Mechanic fan efficiency, η_{mf}	*1*
Adiabatic fan efficiency, η_f	*0.87*
Compressor	
Overall Pressure Ratio, β_c	*13.43*
Mechanic compressor efficiency, η_{mc}	*1*
Adiabatic compressor efficiency, η_c	*0.87*
Combustor	
Turbine Inlet Temperature, *TIT*	*1243 [K]*
Pneumatic combustor efficiency, ε_b	*1*
Combustion efficiency, η_b	*0.9*
High-Pressure Turbine	
Mechanic turbine efficiency, η_{mtH}	*1*
Adiabatic turbine efficiency, η_{tH}	*0.93*
Low-Pressure Turbine	
Mechanic turbine efficiency, η_{mtL}	*1*
Adiabatic turbine efficiency, η_{tL}	*0.93*

Table 2.4. Turbofan input data

2.5.3 Propulsive Performance Characterization

- **Thrust**

Thrust equation is different from previous ones, because two distinct nozzles

are presented. Equation 2.74 second term considers only flow portion that passes through the combustor.

$$T = \dot{m}_c \cdot [(1+f) \cdot w_c + BPR \cdot w_f - (1+BPR) \cdot u] + A_e \cdot (p_e - p_0) \quad (2.74)$$

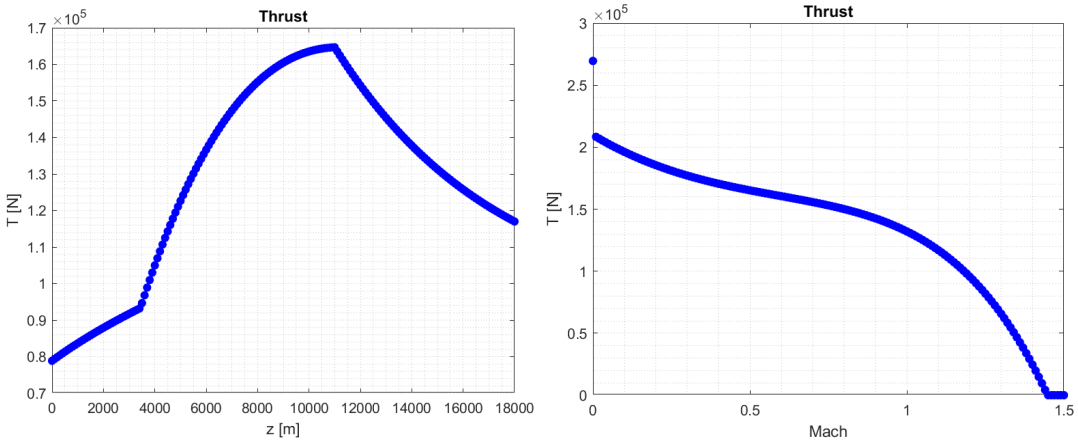

Figure 2.24. thrust varying altitude and Mach

Differently from turbojet, high by-pass ratio turbofan operates well for the lowest Mach numbers; Figure 2.24 shows that maximum thrust value is around $M = 0$.

- **Specific Thrust**

$$I_a = \frac{T}{\dot{m}_0} = \frac{(1+f) \cdot w_c + BPR \cdot w_f - (1+BPR) * u}{1+BPR} \quad (2.75)$$

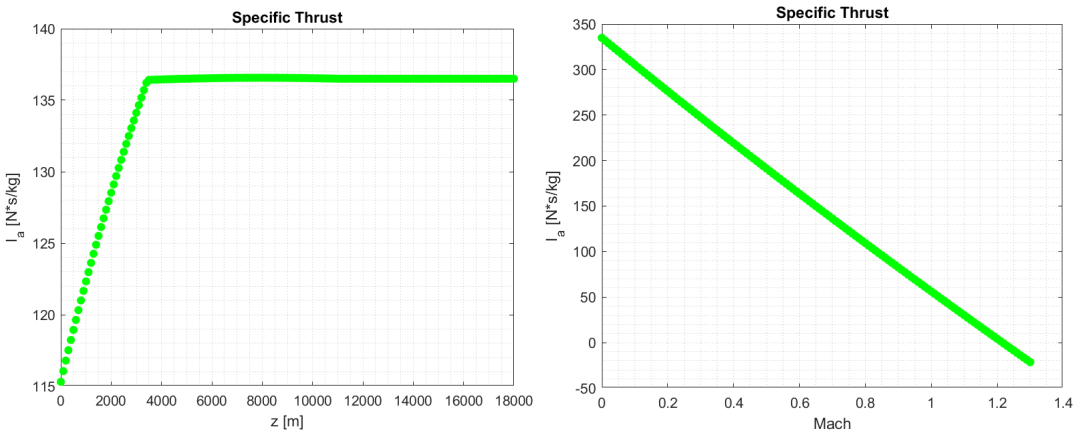

Figure 2.25. specific thrust varying altitude and Mach

- **Thrust Specific Fuel Consumption**

$$I_{sp} = \frac{\dot{m}_b}{T} \tag{2.76}$$

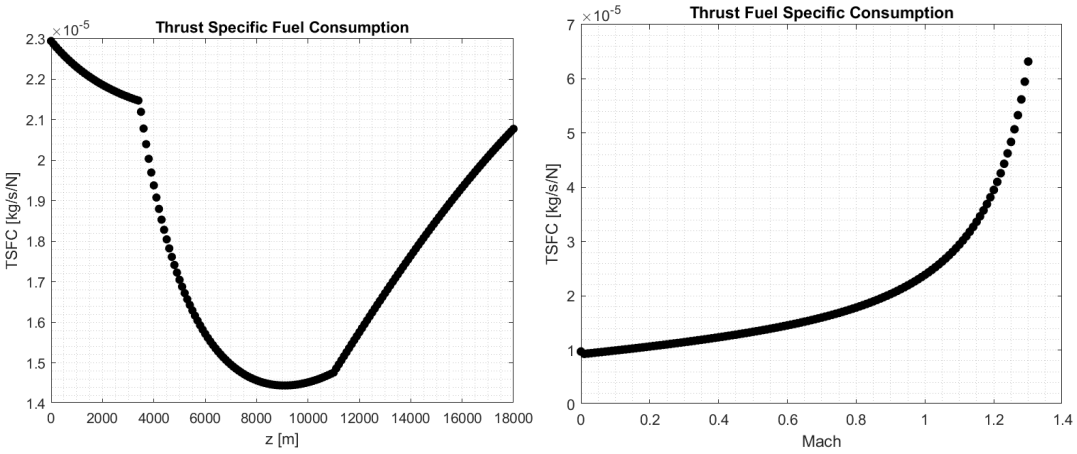

Figure 2.26. Olympus 593 TSFC varying altitude and Mach

2.5.4 Mixed-Flow Turbofan

Mixed-flow turbofan or low by-pass ratio turbofan are different from the separated-flow ones because they are normally characterized by a lowest *BPR* but also because they're different nozzle configuration.
'Mixing is essential for an afterburning turbofan when maximum thrust boosting is required, to avoid the need for two reheat combustion systems. Thanks to the process it's useful for supersonic flight, but in certain cases mixing may also be advantageous in subsonic transport applications, giving a small but significant gain in TSFC.' [4]

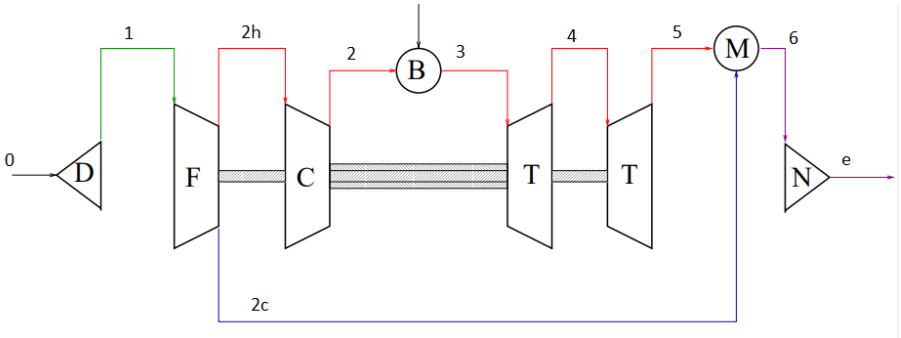

Figure 2.27. Mixed-flow turbofan thermodynamic cycle [5]

As shown in Figure 2.27, flow coming from combustion chamber ('hot' flow) and from fan ('cold' flow) are mixed together and expanded in the common nozzle.
Thermodynamic process is equal to the precedent one; however, mixer imposes new conditions of static pressure that ,if no swirl are presented, can be summarized with:

$$p_6 = p_5 = p_{2c} \tag{2.77}$$

Which can be reported approximately also to total pressure.
Second condition from the enthalpy balance imposed:

$$(\dot{m}_h + \dot{m}_c + \dot{m}_b) \cdot c_p' \cdot T_6^0 = \dot{m}_c \cdot c_p \cdot T_{2c}^0 + (\dot{m}_h + \dot{m}_b) \cdot c_p' \cdot T_5^0 \tag{2.78}$$

From Equation 2.78, T_6^0 can be found, and finally exit speed as in Equation 2.24.

Another difference with separated-flow configuration regarded available data; in fact, Equation 2.77 imposed connection between *BPR* and *FPR* values. Sometimes

[4] HIH Saravanamuttoo, GFC Rogers, H Cohen, *GAS TURBINE THEORY*, PEARSON

only one of them are specified in constructor's data, so the other can be calculated thanks to the following equation, obtained through thermodynamic cycle analysis.

$$(1+f)\cdot\eta_{mt}\cdot\eta_t\cdot\frac{TIT}{T_0}\cdot\left[1-\left(\frac{1}{\eta_b\cdot\beta_c}\right)^{\frac{\gamma-1}{\gamma}}\right]=$$
$$=\left(1+\frac{\gamma-1}{2}\cdot M_0^2\right)\cdot\left[(1+BPR)\cdot\frac{FPR^{\frac{\gamma-1}{\gamma}}-1}{\eta_f\cdot\eta_{mf}}+\left(1+\frac{FPR^{\frac{\gamma-1}{\gamma}}-1}{\eta_f}\right)\cdot\frac{\beta_c^{\frac{\gamma-1}{\gamma}}-1}{\eta_c\cdot\eta_{mc}}\right] \tag{2.79}$$

After FPR and w_e calculation, low by-pass ratio turbofan can be treated as the previous one.

2.6 Input data obtaining

[3, 1] Models presented in this chapter represent the classic thermodynamic cycle utilised nowadays for subsonic and supersonic cruise; thanks to them, thrust and the other outputs can be useful during a preliminary conceptual design analysis.
This method effectiveness is limited by amount od inputs data available for users. Certainly, if engine values are known, they will be used; *ICAO engine database* can be useful to find data of old and modern engine, from turbojet to turbofan: it contains especially compression data and engine dimensions.
Another possibility can be statistical analysis evaluation or, for turbofan engine (most modern engine, for which data are not so available), approximation method, such as "Turbofan engine database as a preliminary design tool" by C. Svoboda.[5]. Thanks to this method, inlet air mass flow, total pressure ratio and by-pass ratio can be found, knowing one of the following parameters: engine dry weight, fan or nacelle diameter, or engine length.
Other important parameters that have to be known for these type of analysis are efficiency and losses. These data can be found in literature, for every engine class. In Table 2.5[6] there turbofan efficiency for various technology development; the levels of technology can be thought of as representing the technical capability for 20-year increments in time beginning in 1945. Thus level 3 technology presents typical component design values for the time period 1985-2005.

[5]Charlie Svoboda, *Turbofan engine database as a preliminary design tool*, Department of Aerospace Engineering, The University of Kansas, 2004 Learned Hall, Lawrence, KS 66045, USA

[6]Jack D. Mattingly, William H. Heiser, David T. Pratt, *Aircraft Engine Design*, American Institute of Aeronautics and Astronautic, Second Edition

		Level of technology			
Component	**Type**	**1**	**2**	**3**	**4**
Diffuser	Subsonic	0.90	0.95	0.98	0.99
	Supersonic	0.88	0.93	0.96	0.97
Compressor	-	0.80	0.84	0.88	0.90
Fan	-	0.78	0.82	0.86	0.89
Burner	-	0.88	0.94	0.99	0.99
Turbine	-	0.80	0.85	0.89	0.91
Nozzle	Convergent	0.93	0.96	0.97	0.98
	Divergent	0.90	0.93	0.95	0.98
Afterburner	-	0.85	0.91	0.96	0.97

Table 2.5. Components efficiency for total pressure losses

In Table 2.6[7] maximum temperature that turbine or nozzle materials can tolerate is presented.

	Level of technology			
Feature	**1**	**2**	**3**	**4**
Maximum turbine T [K]	1110	1390	1780	2000
Maximum afterburner T [K]	1390	1670	2000	2220

Table 2.6. Components maximum temperature tolerance

[7]Jack D. Mattingly, William H. Heiser, David T. Pratt, *Aircraft Engine Design*, American Institute of Aeronautics and Astronautic, Second Edition

Chapter 3

Hypersonic Models Development

[22, 23, 19] This chapter aims toward development and explanation of air-breathing engine models for hypersonic vehicle.
STRATOFLY project has been funded by the European Commission, under the framework of Horizon 2020 plan, with the aim of studying potential of civil high-speed aircraft, respecting technical, environmental and economic viability. In particular, STRATOFLY MR3 vehicle concept allows 300 passengers to move between places located at the antipodes in few hours, reaching Mach 8 cruise speed. The H2020 STRATOFLY Project is based on LAPCAT MR2.4 vehicle so, also engines design refers to LAPCAT 2 concept.
Propulsion system design starts with conceptual analysis and integration of two different combined engine: 6 Air Turbo Rocket (ATR) and the Dual Mode Ramjet (DMR) and related inlet and outlet ducts. ATR is a rocket based air-breathing engine which are responsible to propel the aircraft from take-off till high-supersonic cruise speed (up Mach 4). After reaching first cruise speed of Mach between 4 and 4.5, ATR engines are shut down and the aircraft is only being propelled by DMR engine. The Dual Mode Ramjet is an air-breathing engine that can work in a ramjet configuration (subsonic combustion) or in scramjet one (supersonic combustion), varying conduits geometry and properties during flight. These different configurations are useful because DMR is also utilised after Mach 1.5 to contribute the thrust level during the supersonic acceleration.
The incoming air is taken inside the propulsion duct from the common ATR-DMR intake, then it is split up by two; core flow goes to DMR engine combustor and other part passes to right and left ATR engines bays. After incoming air is burned in one the two engines combustion chamber, the exhaust gas is ejected in the common nozzle section. Air ingested by intake can also by-pass one of the unused engine in that specific flight regime.

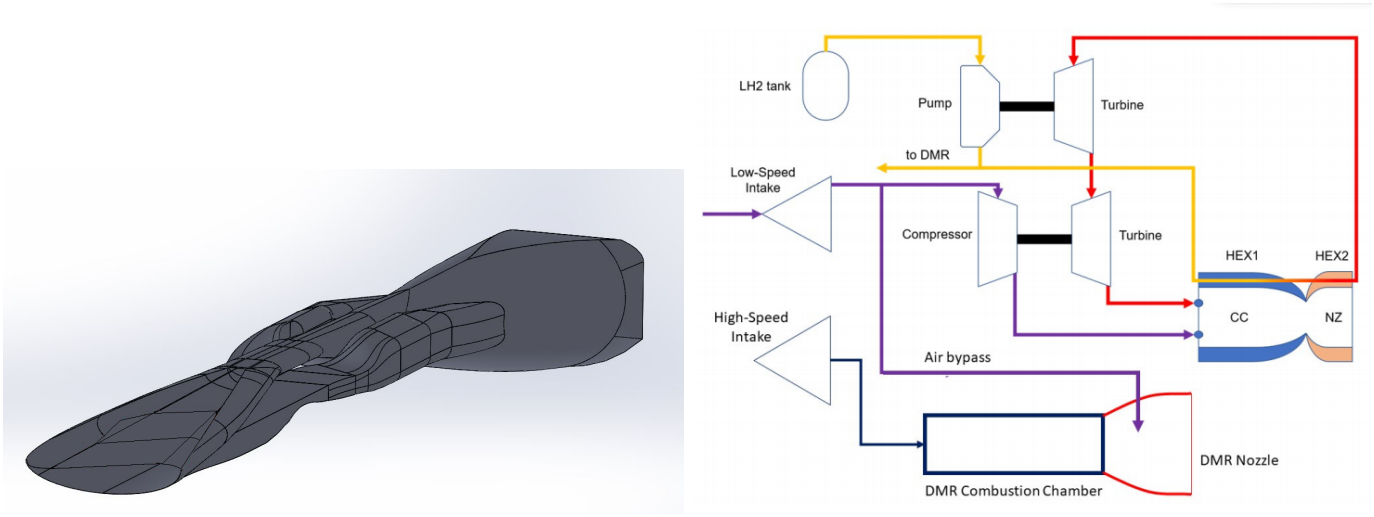

Figure 3.1. ATR and DMR of STRATOFLY MR3

In Figure 3.2 propulsion plant of combined engine is presented.

- **10 - 21**: common intake for DMR and ATR, even though it is useful for DMR.
- ATR conduit:
  - **21 - 211**: low speed intake LSI for ATR.
  - **211 - 81**: between these two sections ATR engine is placed.
  - **81 - 812**: low speed nozzle.
- **812 - 100**: common nozzle for DMR and ATR, even though it is useful for DMR.
- DMR conduit:
  - **10 - 20**: high speed intake HSI for DMR.
  - **20 - 80**: DMR engine.
  - **80 - 802**: first expansion high speed nozzle.
  - **802 - 100**: second expansion high speed nozzle; this permits the last gas acceleration to reach the hypersonic speed.

Geometry data are fundamental to analyse both engine thermodynamic cycle. However, not every models will use all the stations area inputs; this difference will affect results of course, but if a minor quantity of data are found in literature, user can obtain some results. The same argument can be done for others inputs presented after, such as combustion temperature.

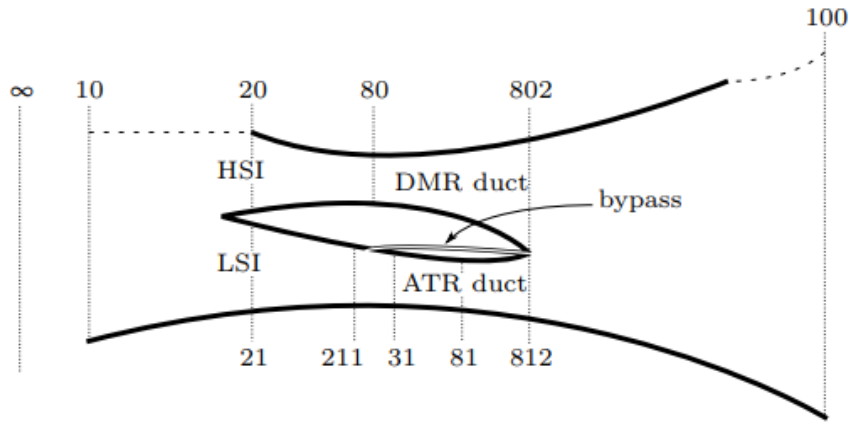

Figure 3.2. ATR and DMR scheme and stations numbering [14]

Station	21	211	31	81	812
A $[m^2]$	10.9	19.1	19.1	17.4	20.6

Station	10	20	80	802	100
A $[m^2]$	37.7	7.3	4.9	15.9	111.2

Table 3.1. ATR and DMR propulsion plant

The most important aim of the thesis work is to develop models for hypersonic vehicle, starting from the classic engine mock-up presented in the previous chapter and trying to adapt them to the different concept. In the following subsections, different solutions of these two engine will be shown.

3.1 Air Turbo Rocket

Air Turbo Rocket is a particular turbine-engine combined cycle with high thrust-to-weight ratio and specific thrust; it combines elements of turbojet and rocket motors.
[17, 14] In Figure 3.4, ATR model is presented: the free-stream in firstly compressed by the intake and then by the fan, that permits major compression during low-speed phases, where the pressurization due to inlet won't be sufficient. Compressed air is finally sent to the combustion chamber.
On the other hand, fuel-cycle takes place: liquid hydrogen is stored at pressure and temperature respectively of 3 bar and 20 K, kept at the correct pressure thanks to a specific turbo-pump and at the correct temperature with the regenerative heat exchanger located around combustor. Fuel is sent to combustion chamber using

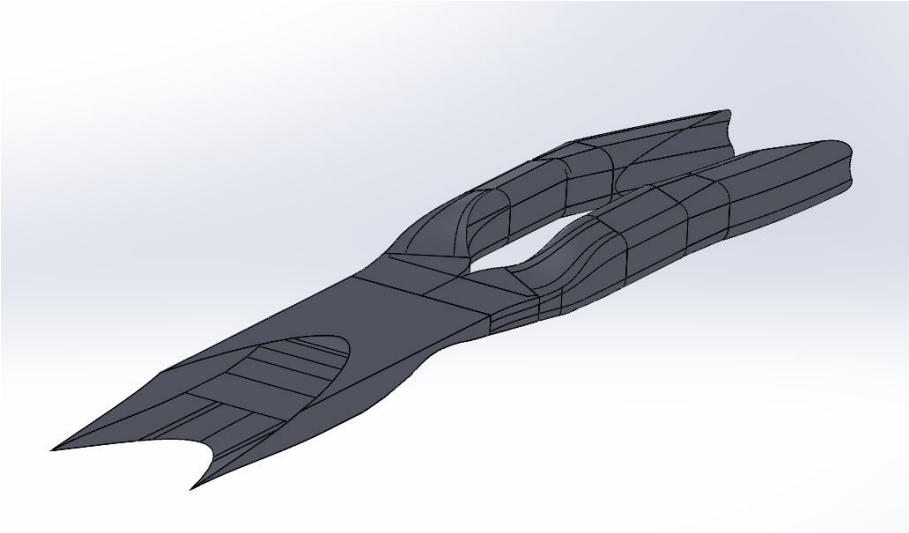

Figure 3.3. ATR STRATOFLY MR3 external structure

turbine, which drive both the pump and the fan. Finally, combustion takes place and flow is discharged through the nozzle.

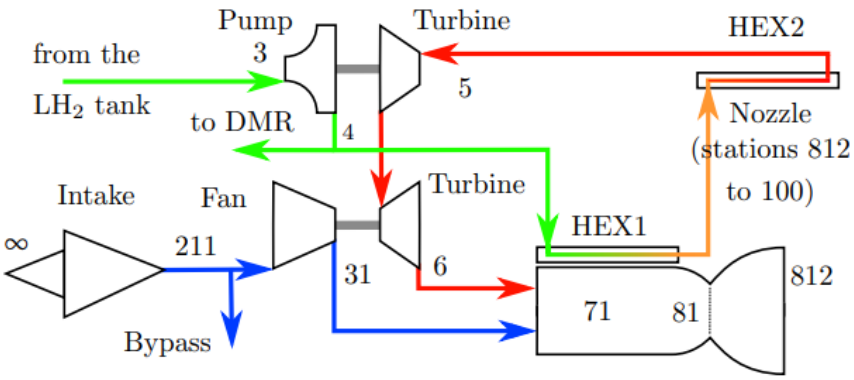

Figure 3.4. ATR expander cycle of STRATOFLY MR3 [14]

3.1.1 Ramjet with Compressor Model

First and the simplest model built is based on ramjet thermodynamic cycle, analysed in the previous chapter. Referring to Figure 3.4, if air flow is follow through the engine, the only elements found are the intake, the compressor and final combustor-nozzle group. So, starting from ramjet model, a compression stage is added after

the intake.
This model is analysed between station 21 and 812 of Figure 3.2. The only section area geometry useful is the LSI area; firstly, no temperature after combustion data are required, but only the air-fuel ratio has been inserted (supposed equal to stoichiometric value).

- **Intake**
  Differently from classic thermodynamic cycle analysed before, $\dot{m}_0$ is not directly known, but it can be obtained from intake area A_0, using also atmosphere model.

$$\dot{m}_0 = A_0 \cdot \rho_0 \cdot u \tag{3.1}$$

  Where u is the free-stream speed.
  As for ramjet cycle, intake is characterised by pneumatic efficiency ε_d.

$$T^0_{211} = T^0_0 \tag{3.2}$$

$$p^0_{211} = \varepsilon_d \cdot p^0_0 \tag{3.3}$$

- **Compressor**
  Fan stage is posed between stations 211 and 31. Overall Pressure Ratio OPR is supposed equal to 6, classic value for medium turbojet compressor stages. The adiabatic compressor efficiency η_c is supposed equal to 0.8.

$$T^0_{31} = T^0_{211} \cdot [1 + \frac{1}{\eta_c} \cdot (OPR^{\frac{\gamma-1}{\gamma}} - 1)] \tag{3.4}$$

$$p^0_{31} = OPR \cdot p^0_{211} \tag{3.5}$$

- **Combustion chamber**
  Differently from subsonic and supersonic engine, temperature after combustion is not a data so easy to find. Starting from stoichiometric fuel ratio ($f_{st} = 0.029$ for Liquid Hydrogen), temperature after combustion T^0_{81} can be found from combustor balance equation.

$$\eta_b \cdot \dot{m}_b \cdot H_i = (\dot{m}_0 + \dot{m}_b) \cdot c'_p \cdot (T^0_{81} - T^0_{31}) \tag{3.6}$$

  Where fuel flow ratio $\dot{m}_b = \dot{m}_0 \cdot f$, adiabatic combustor efficiency η_b is equal to 0.9, heats of reaction of Liquid Hydrogen $H_i = 120.9[J/kg]$ and combusted gases specific heat $c'_p = 1900[J/(kg * K)]$. From Equation 3.6:

$$T_{81}^0 = T_{31}^0 + \eta_b \cdot f \cdot \left(\frac{H_i}{c'_p}\right) \tag{3.7}$$

In this way, combustion temperature will increase with Mach number, that what is normally happened in supersonic and hypersonic flight. Supposing pneumatic combustor efficiency equal ε_b to 0.95, total pressure after combustion is also found.

$$p_{81}^0 = \epsilon_b \cdot p_{31}^0 \tag{3.8}$$

- **Nozzle**
  In this first traction engine nozzle is considered adapted; with this solution, nozzle area won't be requested as known data. Exit values can be calculated, simply supposing pneumatic nozzle efficiency ε_n.

$$T_{812}^0 = T_{81}^0 \tag{3.9}$$

$$p_{812}^0 = \varepsilon_n \cdot p_{81}^0 \tag{3.10}$$

Finally, exit flow speed w_e:

$$w_e = \sqrt{2 \cdot c'_p \cdot T_{812}^0 \cdot \left[1 - \left(\frac{p_0}{p_{812}^0}\right)^{\frac{\gamma'-1}{\gamma'}}\right]} \tag{3.11}$$

A different possibility is that combustion temperature is known or it can be obtained. In this case, from combustor balance equation 3.6, f is calculated and it is supposed constant with Mach number increasing. No other changes are done in cycle presented before.

3.1.2 Turbojet and Ramjet Model

This second model uses more fidelity classic thermodynamic cycle of the previous chapter, especially for the lowest Mach number. Ramjet model is not so correct for subsonic and for low supersonic, because ramjet won't be useful in these flight regimes, even though the compressor stages will guarantee a major air flow to combustor if the air mass speed coming from intake is not sufficient. Despite using ramjet with compressor model for all the Mach values, classic turbojet model is utilised.

- **Turbojet**

  Turbojet model is utilised for $0 < M_0 \leq 2.5$.
  Previous chapter single-spool turbojet engine is implemented.

  – **Intake**
  Values after intake compression are estimated knowing intake pneumatic efficiency ε_d.

$$T^0_{211} = T^0_{21} = T^0_0 \tag{3.12}$$

$$p^0_{211} = \varepsilon_d \cdot p^0_0 \tag{3.13}$$

  – **Compressor**
  Overall Pressure Ratio OPR is supposed equal to 1.5, as MR3 ATR fan pressure ratio.

$$T^0_{31} = T^0_{211} \cdot [1 + \frac{1}{\eta_c} \cdot (OPR^{\frac{\gamma-1}{\gamma}} - 1)] \tag{3.14}$$

$$p^0_{31} = OPR \cdot p^0_{211} \tag{3.15}$$

  – **Combustor**
  Combustor balance equation is the same of 3.6. Differently from classic turbojet cases, temperature after combustion (corresponding to Turbine Inlet Temperature TIT) is evaluated, starting from stoichiometric ratio $f_{st} = 0.029$.

$$TIT = T^0_{81} = T^0_{31} + \eta_b \cdot f \cdot \left(\frac{H_i}{c'_p}\right) \tag{3.16}$$

  And also total pressure can be calculated through the same combustor pneumatic efficiency ε_b.

$$p^0_{81} = \epsilon_b \cdot p^0_{31} \tag{3.17}$$

  – **Turbine**
  Turbine machine can be hypothetically posed between combustion chamber and nozzle, in section **81 - 811**.
  From balance equation of power between turbine and compressor, expansion turbine ratio β_t is calculated, knowing compressor and turbine mechanic efficiencies.

$$\beta_t = \frac{1 - c_p \cdot (T_{31}^0 - T_{211}^0)}{c_p' \cdot \eta_{mc} \cdot \eta_{mt} \cdot \eta_t \cdot (1+f) \cdot T_{81}^0}^{\frac{-\gamma'}{\gamma'-1}} \tag{3.18}$$

Thanks to β_t, exit turbine values of temperature and pressure can be obtained.

$$T_{811}^0 = T_{81}^0 - \frac{c_p}{c_p'} \cdot \frac{1}{\eta_{mt} \cdot \eta_{mc}} \cdot \frac{T_{31}^0 - T_{211}^0}{1+f} \tag{3.19}$$

$$p_{811}^0 = \frac{p_{81}^0}{\beta_t} \tag{3.20}$$

– **Nozzle**
Exit conditions are also calculated as single-spool turbojet case; critic pressure is evaluated as in Equation 2.13, exit pressure, Mach number and temperature like in Equations 2.14 - 2.18. The exit flow speed:

$$w_e = M_e \sqrt{(\gamma' \cdot R' \cdot T_e)} \tag{3.21}$$

This model requests more parameters than simple ramjet with compressor one: all the efficiencies and pneumatic losses of turbojet have to be known or supposed, and nozzle exit area is necessary to calculate thrust.

- **Ramjet with Compressor**

Ramjet with compressor model is utilised for $2.5 < M_0 \leq 4$.
It respects exactly thermodynamic cycle presented in the previous subsection.

3.1.3 ATR Completed Model

Last model developed is the most completed, but also the one which need more input data. It starts from the ramjet with compressor model of the previous chapter, where the air mass flow has been treated, and 'fuel part' is added to that simplest thermodynamic cycle.
Referring to Figure 3.4, fuel cycle is described below.

- **Pump**
Fuel is stored at the correct pressure and temperature. Thanks to pump work (treated as a compressor stages), Liquid Hydrogen value can be taken to the correct pressure value for mixing and combustion with air mass flow. Knowing pump compression ratio β_p, adiabatic pump efficiency η_p, propellant adiabatic expansion coefficient γ_{LH} and Liquid Hydrogen specific heat $c_{p_{LH}}$, fuel pressure and temperature can be found.

$$T_4^0 = T_3^0 \cdot [1 + \frac{1}{\eta_p} \cdot (\beta_p^{\frac{\gamma_{LH}-1}{\gamma_{LH}}} - 1)] \tag{3.22}$$

$$p_4^0 = \beta_p \cdot p_3^0 \tag{3.23}$$

Where subscripts *4* indicates values after pump and *3* LH tank values.

- **Turbine**
  Turbine drives both the pump and fan. Turbine pressure ratio β_t is calculated as the expansion value necessary for fan compression.

$$\beta_t = \frac{p_4^0}{p_{31}^0} \tag{3.24}$$

  Thanks to β_t, exit turbine values of fuel temperature and pressure can be obtained.

$$T_6^0 = T_4^0 - \frac{c_p}{c_p'} \cdot \frac{1}{\eta_t} \cdot \frac{T_4^0 - T_3^0}{1+f} \tag{3.25}$$

  Where η_t is adiabatic turbine efficiency, *4* and *6* indicate respectively values before and after turbine expansion.

$$p_6^0 = \frac{p_4^0}{\beta_t} \tag{3.26}$$

- **Mixer**
  Mixer is posed before combustion chamber. As for mixed-flow turbofan case, mixing imposes the same total pressure for propellant and air, while mixer exit temperature or inlet burner temperature is calculated as below.

$$T_{71}^0 = \frac{\dot{m}_0 \cdot c_p \cdot T_{31}^0 + \dot{m}_b \cdot c_{p_{LH}} \cdot T_6^0}{c_p' \cdot (\dot{m}_0 + \dot{m}_b)} \tag{3.27}$$

T_{71}^0 becomes the new inlet combustion chamber temperature for the ramjet with compressor ATR model, replacing T_{31}^0 in Equation 3.4.

$$TIT = T_{81}^0 = T_{71}^0 + \eta_b \cdot f \cdot \left(\frac{H_i}{c_p'}\right) \tag{3.28}$$

Other parts of thermodynamic cycle don't vary from previous model. 'Completed Model' section of the table included the previous 'Ramjet with Compressor Model'.

3.1.4 ATR Input Data

Input data utilised for STRATOFLY MR3 are presented in Table 3.2.

COEFFICIENT	VALUE
Liquid Hydrogen	
Heats of reaction, H_i	*120.9 [MJ/kg]*
Stoichiometric fuel ratio, f_{st}	*0.029*
Propellant adiabatic expansion coefficient, γ_{LH}	*1.4*
Combusted gases adiabatic expansion coefficient, γ'	*1.33*
Propellant specific heat, $c_{p_{LH}}$	*14435 [J/(kg*K)]*
Combusted gases specific heat, c'_p	*1900 [J/(kg*K)]*
Ramjet with Compressor Model	
Overall Pressure Ratio, OPR	*6.0*
Intake area, A_{21}	*10.9 [m^2]*
Pneumatic intake efficiency, ε_d	*0.9*
Adiabatic compressor efficiency, η_c	*0.8*
Pneumatic combustor efficinecy, ε_b	*0.95*
Adiabatic combustor efficiency, η_b	*0.9*
Pneumatic nozzle efficiency, ε_n	*0.98*
Ramjet with Compressor Model (Temperature known)	
Temperature after combustion, T_{81}	*3000 [K]*
Turbojet and Ramjet Model (Turbojet)	
Overall Pressure Ratio, OPR	*1.5*
Intake area, A_{21}	*10.9 [m^2]*
Exit nozzle area, A_{812}	*20.6 [m^2]*
Pneumatic intake efficiency, ε_d	*0.98*
Adiabatic compressor efficiency, η_c	*0.88*
Mechanic compressor efficiency, η_{mc}	*1*
Pneumatic combustor efficinecy, ε_b	*0.95*
Adiabatic combustor efficiency, η_b	*0.9*
Adiabatic turbine efficiency, η_t	*0.8*
Mechanic turbine efficiency, η_{mt}	*0.95*
Pneumatic nozzle efficiency, ε_n	*0.98*
Completed Model	
Overall Pressure Ratio, OPR	*8.0*
Storage fuel temperature, T_3	*20 [K]*
Storage pressure temperature, p_3	*3 [bar]*
Compression pump fuel ratio, β_p	*15*

Table 3.2. STRATOFLY MR3 Air Turbo Rocket input data

3.1.5 ATR Propulsive Performances

In this section, Air Turbo Rocket performances are analysed.
The database for the ATR engine was set up using the specific impulse data by Steelant [18]. From the specific impulse data calculated by VKI for the ATR engine, propulsion database has been obtained. Thrust has been calculated by the intake captured air mass-flow rate depending on the free stream conditions and the set equivalence ratio, as shown in Figure 3.5. This analysis has been based on a CFD analysis of LAPCAT MR2, but it can be considered effective also for STRATOFLY MR 3.

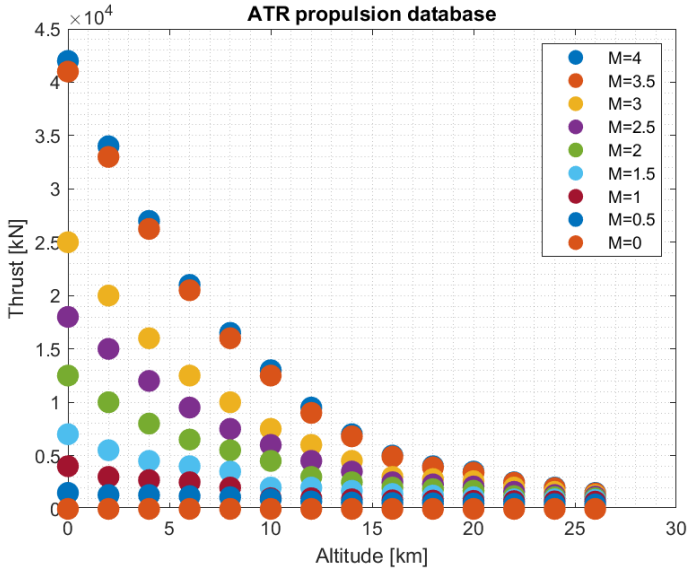

Figure 3.5. STRATOFLY MR3 ATR Propulsive database

- **Thrust**

$$T = \dot{m}_0 \cdot [(1+f) \cdot w_e - u] + A_e \cdot (p_e - p_0) \tag{3.29}$$

Comparing various models in Figure 3.6, results show some differences. Ramjet with compressor model (combustion temperature known) is a little bit underrated, especially for the highest Mach numbers; however, if temperature of combustion is increased (it won't be a realistic solution), it will be the most accurate model for high speed, due to little thrust gain between Mach 3.5 and Mach 4. This model presents additional problems for low speeds, where an overestimation of the thrust can be observed; this effect would be further

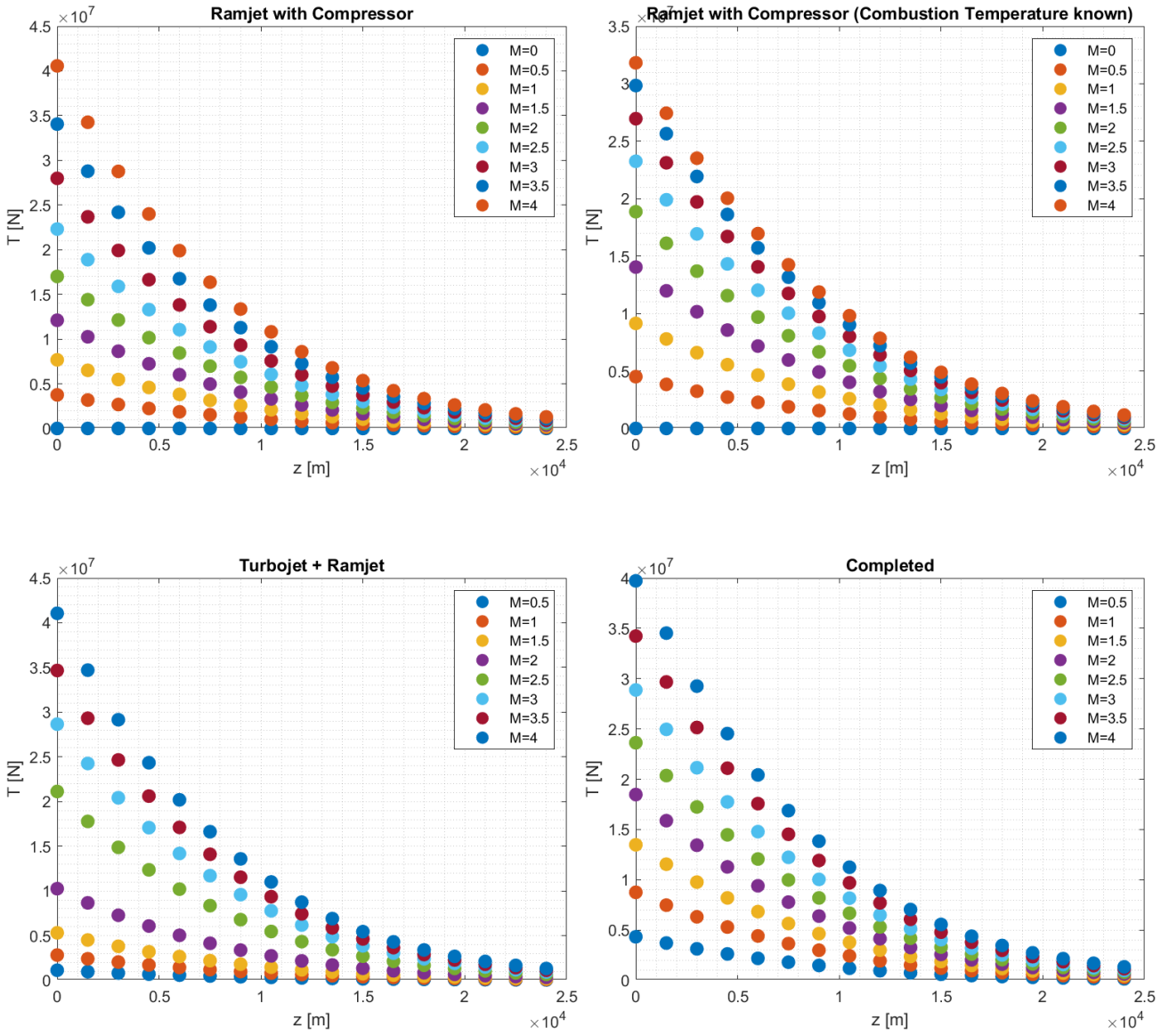

Figure 3.6. STRATOFLY MR3 Air Turbo Rocket Thrust

increased if the end-of-combustion temperature is increased.
The two most representative models of the ATR engine (Ramjet with compressor and Completed models) present very similar results, as the added fuel cycle in the full model does not significantly affect the parameters influencing thrust. The graphs of these two models can nevertheless be considered valid in the conceptual design phase, although the problem of overestimation for low Mach numbers persists. Especially Ramjet with compressor model can be an

optimum candidate, due to the few necessary input data.
The model which results are closest to the propulsion database is the Turbojet + Ramjet model; in fact, it is the only one that faithfully reflects the thrust for low speeds, because the turbojet model is more representative of these flight phases. Its problem concerns the large amount of input required, due to two different engine types enclosed within it.

Differences between ATR performances estimation and ATR database reported in Figure 3.5 can be evaluated as in Equation 3.30.

$$err = \frac{|T_{data} - T_{mod}|}{T_{data}} \tag{3.30}$$

Figure 3.7 shows that both Ramjet with Compressor models overrate engine performances especially for the lowest Mach numbers, between 0.5 and 2. The same trend can be observed also for the Completed model, while Turbojet + Ramjet model shows a better representation during subsonic and supersonic fight regimes, even if the error increases with altitude.

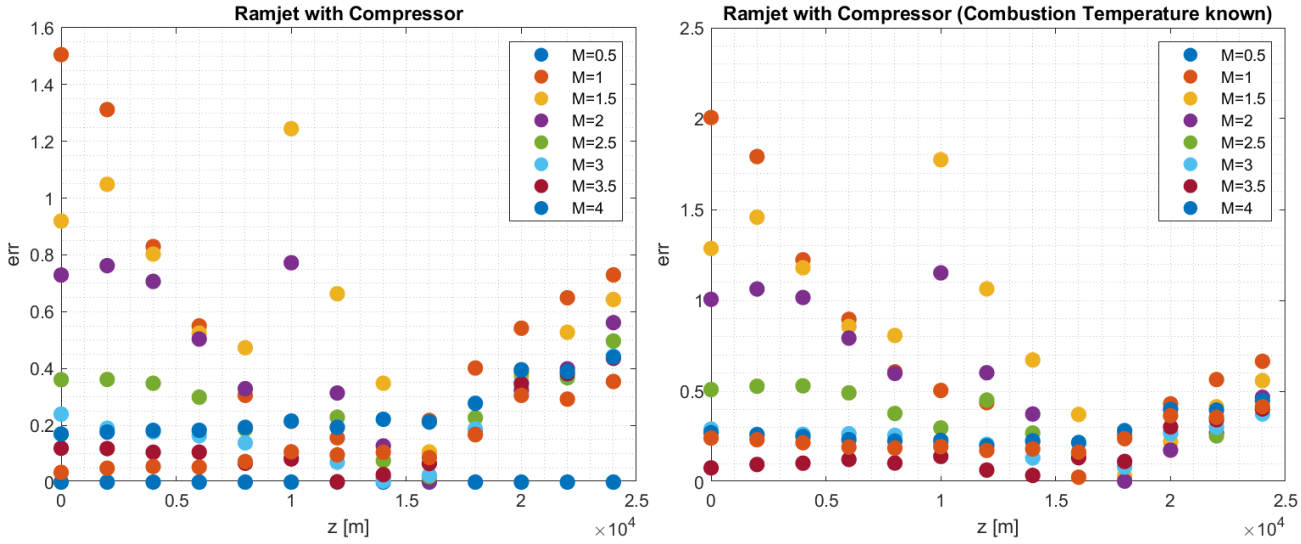

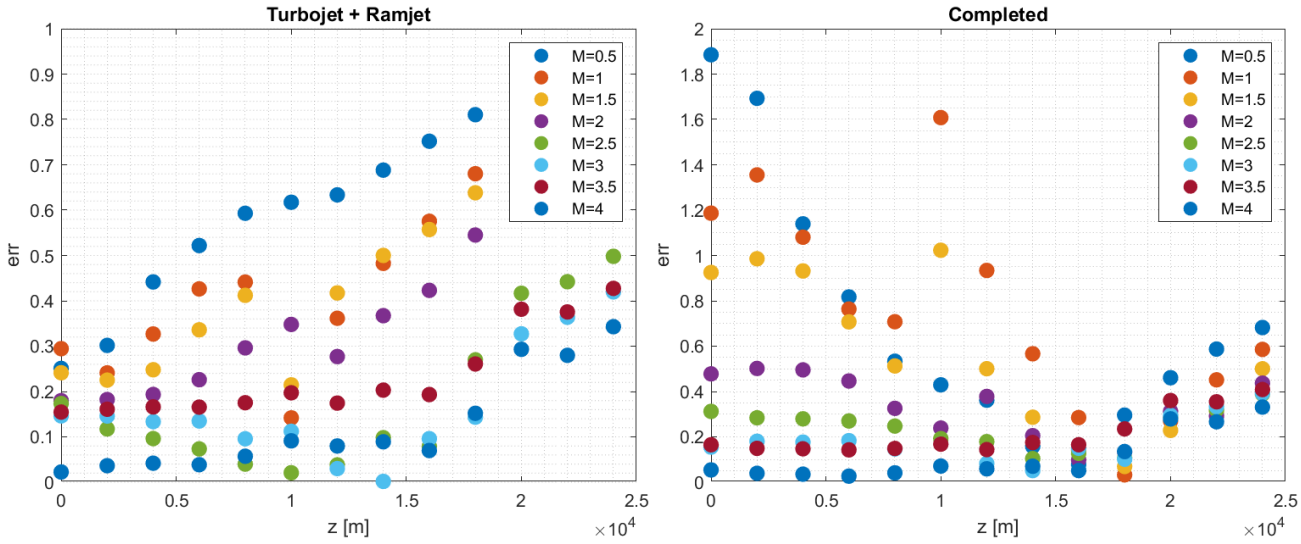

Figure 3.7. Error estimation between ATR database and different models

- **Specific Thrust**

  Regarding Specific Thrust and Specific Thrust Fuel Consumption, even if there is no reference database as for thrust, knowledge of their trend can be useful during the early stages of aircraft design.

$$I_a = \frac{T}{\dot{m}_0} \tag{3.31}$$

  The specific thrust shows an increasing trend with the Mach number in all cases, with the exception of the Ramjet with compressor model with known temperature; in this last case, since the end combustion temperature is fixed, there is no increase in temperature in relation to the speed of the incoming air flow.
  In the other models, specific thrust increases more than the input air flow rate; the largest increase in the Turbojet + Ramjet model occurs around the Mach number at which the transition between the two methods occurs.

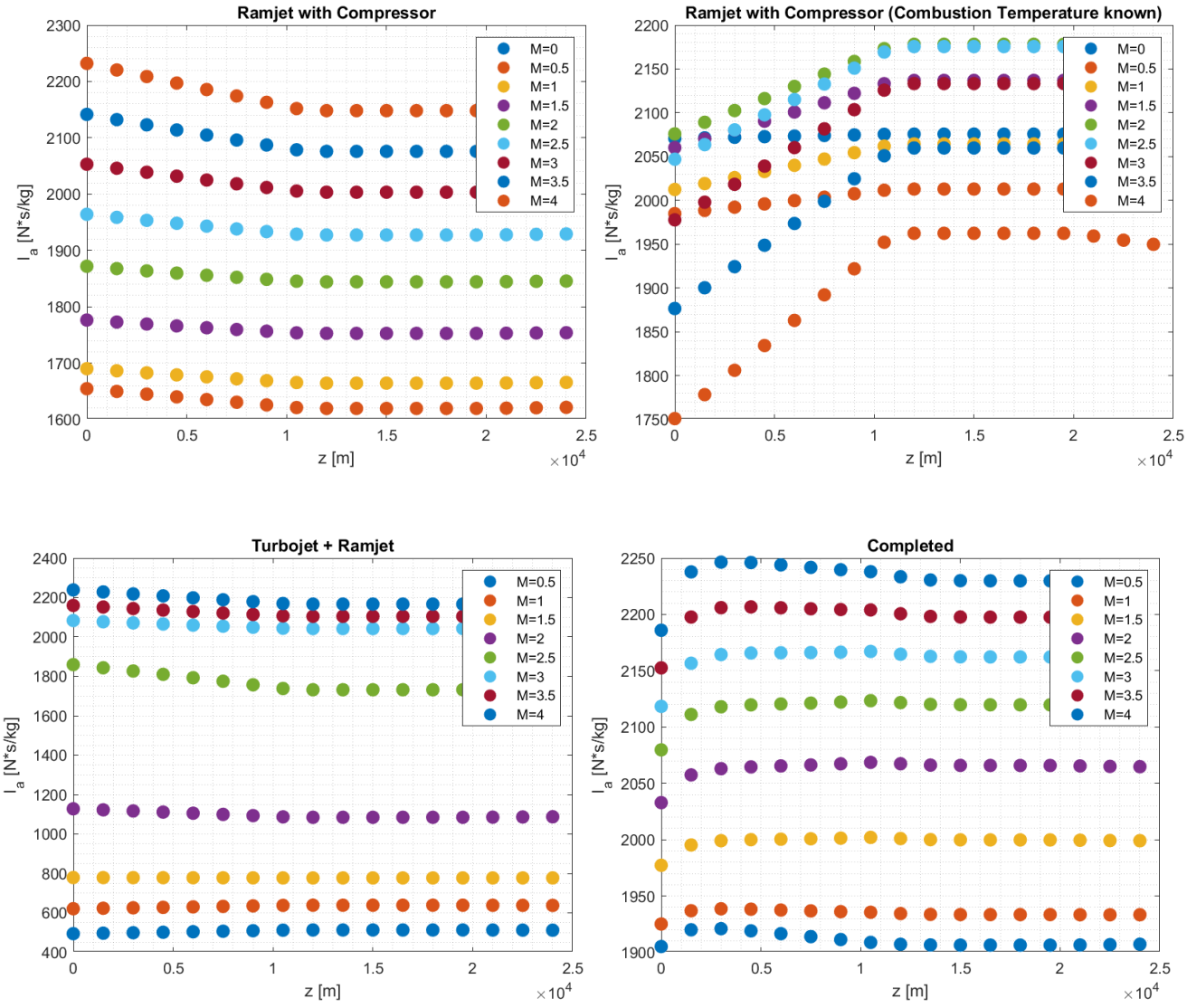

Figure 3.8. STRATOFLY MR3 Air Turbo Rocket Specific Thrust

- **Thrust Specific Fuel Consumption**

$$I_{sp} = \frac{\dot{m}_b}{T} \tag{3.32}$$

Differently from specific thrust, TSFC decreases with increasing Mach number, due to the fact that the thrust increases more than the fuel flow rate (linked to the air flow rate by the air-fuel ratio f). In this case, the trend is respected

also in the model with fixed end combustion temperature because the fuel flow rate is related to f, which is modified step by step by balance combustor equation.

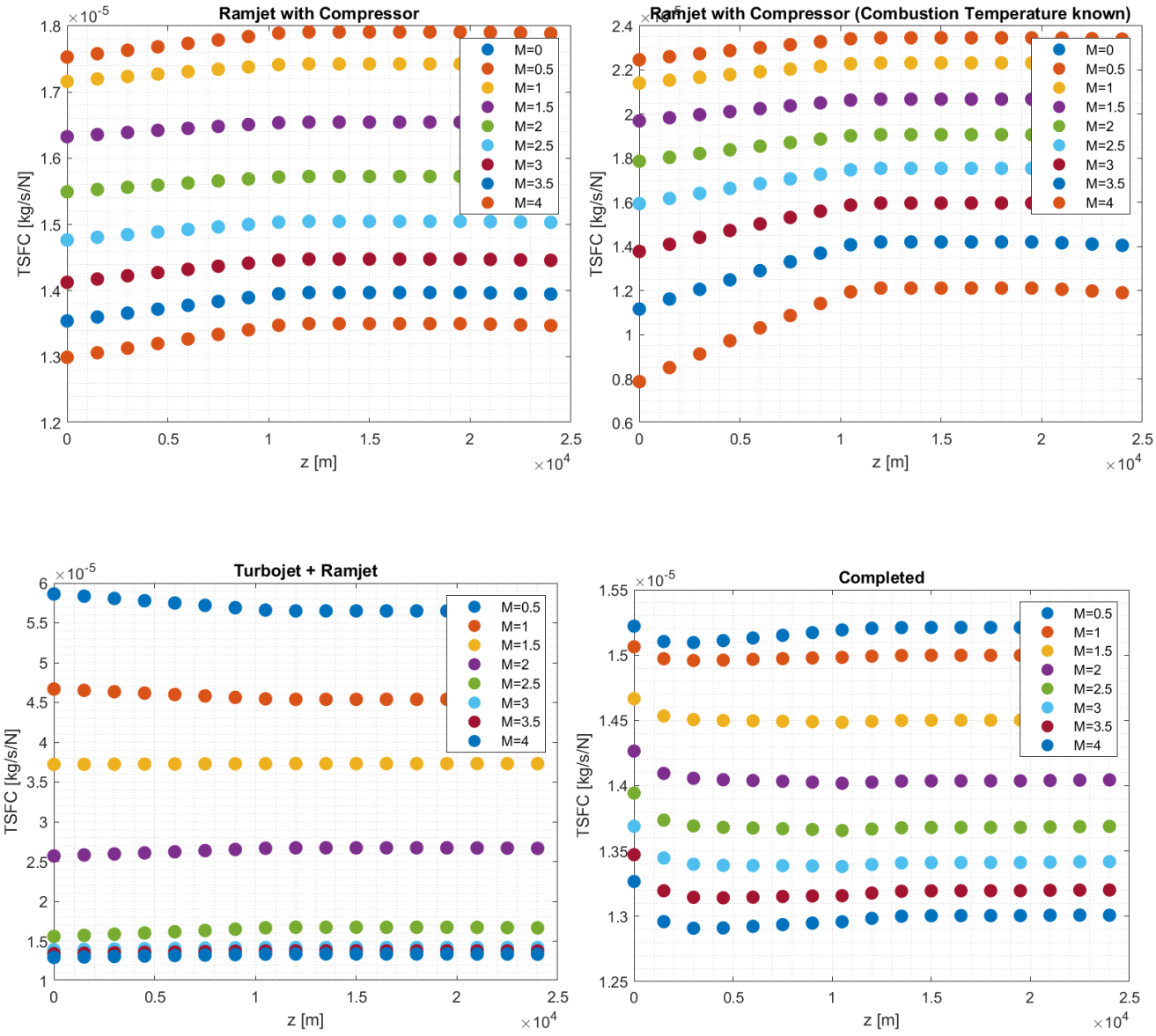

Figure 3.9. STRATOFLY MR3 Air Turbo Rocket Thrust Specific Fuel Consumption

The level of accuracy of the results is always to be considered for a conceptual design analysis, both for ATR and DMR.

3.2 Dual-Mode Ramjet

[21, 14, 17, 23, 18] Dual-Mode Ramjet permits vehicle acceleration from Mach 4 up to Mach 8 and keeps the hypersonic speed during cruise phase. DMR operates in two different configuration: for the lowest Mach number flight, throat area works in slightly supersonic regime, so quite similar to ramjet propulsion; the throat Mach number increases with flight speed and DMR works in supersonic combustion, so like a scramjet, necessary to avoid excessive intake and conduit losses due to high speed flow. For simplicity, models developed are not considering supersonic combustion, treating the entire thermodynamic cycle as ramjet one, with maximum throat Mach number equal to 1.

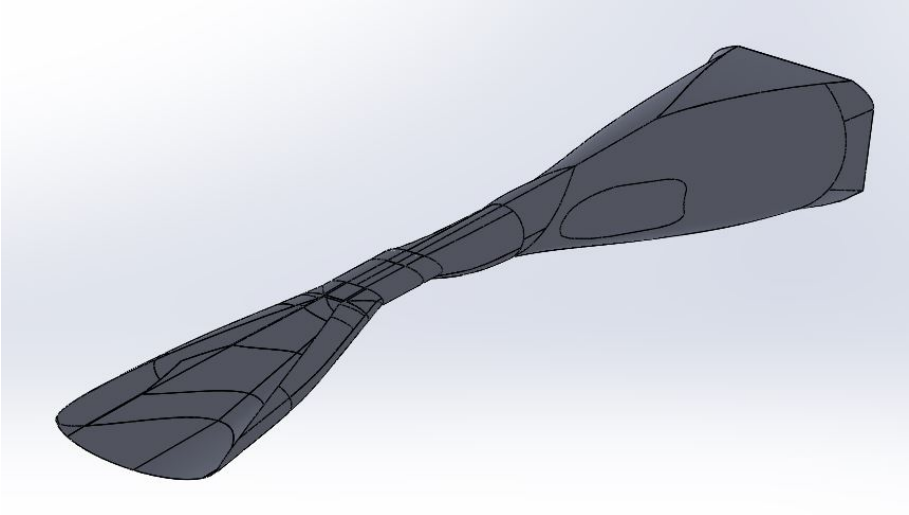

Figure 3.10. DMR STRATOFLY MR3 external structure

Figure 3.2 is used as reference for the next treatment.

3.2.1 Simple Ramjet Model

This first model is based on ramjet treatment presented in the previous chapter. Necessary input are the most basilar ones.

- **Intake**
  Knowing free-stream condition (indicated with subscript *0*) and inlet area A_{10}, intake mass flow rate can be evaluated as for ATR ramjet with compressor case.

$$\dot{m}_{10} = A_{10} \cdot \rho_0 \cdot u \tag{3.33}$$

The equation presented before doesn't take in count of mass flow losses called '*spillage effect*', indicated with ε_{spil}. This effect is due to inlet geometry and it will be explain better after. So, the new air mass flow rate is:

$$\dot{m_{20}} = \varepsilon_{spil} \cdot \dot{m_{10}} \tag{3.34}$$

After air mass flow calculation, others total magnitudes can be evaluated.

$$T_{20}^0 = T_{10}^0 = T_0^0 \tag{3.35}$$

$$p_{20}^0 = \varepsilon_d \cdot p_{10}^0 \tag{3.36}$$

Where ε_d is the intake pneumatic efficiency.

- **Combustion Chamber**
  As in previous cases, from Equation 3.6, f can be found, knowing temperature after combustion T_{80}^0.

$$f = \frac{c_p' \cdot (T_{80}^0 - T_{20}^0)}{\eta_b \cdot H_i - c_p' \cdot (T_{80}^0 - T_{20}^0)} \tag{3.37}$$

  In high supersonic and hypersonic regimes, temperature after combustion can't be derived starting from stoichiometric fuel ratio value because, as shown in Equation 3.7, ending combustion temperature is function of Mach number; so, for the highest flight speed, temperature will be too much big and it will assume unreal value. For the same reason, f is under-limited to a common value.
  Total pressure is found as follow.

$$p_{80}^0 = \varepsilon_b \cdot p_{20}^0 \tag{3.38}$$

  Where ε_b is burner pneumatic efficiency.

- **Nozzle**
  This first and simplest ramjet treatment considers adaptive nozzle. Exit flow speed is calculated without geometry data, but only knowing exit total temperature and pressure.

$$T_{100}^0 = T_{802}^0 = T_{80}^0 \tag{3.39}$$

$$p_{100}^0 = \varepsilon_n \cdot p_{80}^0 \tag{3.40}$$

Where ε_n is nozzle pneumatic efficiency.

Finally, exit flow speed w_e:

$$w_e = w_{100} = \sqrt{2 \cdot c'_p \cdot T^0_{100} \cdot \left[1 - \left(\frac{p_0}{p^0_{100}}\right)^{\frac{\gamma'-1}{\gamma'}}\right]} \tag{3.41}$$

3.2.2 Completed Ramjet Model

[5, 18] Differently from previous one, this thermodynamic cycle takes count on expansion through the nozzle. It is based on hypothesis that consider engine working as a total pressure constant cycle, supposing low speed flow inside it.
Completed ramjet model requires more input than the simplest one, such as throat area and nozzle DMR area; this is due to non adapted nozzle condition that is evaluated thanks to this method.
Stations numbering refers to Figure 3.2.

- **Intake**
  As before, starting from free-stream condition (indicated with subscript *0*) and inlet area A_{10}, intake mass flow rate can be evaluated, considering also spillage effect ε_{spil}.

  $$\dot{m}_{10} = \varepsilon_{spil} \cdot A_{10} \cdot \rho_0 \cdot u \tag{3.42}$$

  After air mass flow calculation, others total magnitudes can be evaluated.

  $$T^0_{20} = T^0_{10} = T^0_0 \tag{3.43}$$

  $$p^0_{20} = \varepsilon_d \cdot p^0_{10} \tag{3.44}$$

  Where ε_d is the intake pneumatic efficiency.

- **Combustion Chamber**
  As in simple ramjet model, from Equation 3.6, f can be found as in Equation 3.37; also in this case, fuel ratio is under-limited.
  Total pressure is found in the same way.

  $$p^0_{80} = \varepsilon_b \cdot p^0_{20} \tag{3.45}$$

  Where ε_b is burner pneumatic efficiency.
  As Figure 3.2 shows, combustion chamber ending corresponds to DMR throat area.

- **Nozzle**
  In this treatment flow is considered isentropic. During this most completed analysis, the nozzle must also be considered not always adapted. In fact, fixing exit and throat area ratio, there is only one condition of exit Mach value that permits nozzle adaptation (in a convergent-divergent conduit).
  Exit Mach number can be evaluated with the following equation.

$$\frac{A_{802}}{A_{80}} = \frac{1}{M_{802}} \cdot \left(\frac{1 + \frac{\gamma'-1}{2} \cdot M_{802}^2}{\frac{\gamma'+1}{2}} \right)^{\frac{\gamma'+1}{2 \cdot (\gamma'-1)}} \tag{3.46}$$

  This treatment limit regard throat Mach number M_{802}, that is always been consider sonic; this is true only for ramjet configuration. However, results will show exit Mach value very similar to the CFD database analysis.
  The same equation 3.46 can be used to evaluate final exit Mach number, only without considering throat Mach equal to 1.

$$\frac{A_{100}}{A_{802}} = \frac{M_{802}}{M_{100}} \cdot \left(\frac{1 + \frac{\gamma'-1}{2} \cdot M_{100}^2}{1 + \frac{\gamma'-1}{2} \cdot M_{802}^2} \right)^{\frac{\gamma'+1}{2 \cdot (\gamma'-1)}} \tag{3.47}$$

  In this way, exit Mach flow number M_{100} can be found. From this value, temperature and exit speed are calculated.

$$T_{100} = \frac{T_{80}^0}{1 + \frac{\gamma'-1}{2} \cdot M_{100}^2} \tag{3.48}$$

$$w_e = w_{100} = M_{100} \sqrt{(\gamma' \cdot R' \cdot T_{100})} \tag{3.49}$$

3.2.3 Simple Ramjet Model with Temperature Variation

The last model implemented is the same of the first one presented in this chapter (simple ramjet model) with variation during combustion chamber process.
As said before, combustion temperature grown gradually with Mach number increasing; however, Equation 3.7 won't be useful for hypersonic flight speed, because of extremely grown of temperature, that will exceed normal values. This model tries to evaluate possible solution of the problem, increasing step by step combustion temperature, every time that thrust value becomes more little than the one at the previous Mach. This solution can be consider as a sort of rudimentary throttle: if combustion temperature is not enough to reach desirable speed, it will be grown (for example thanks to fuel addition).
Formula utilised for temperature after combustion increasing is the follow one.

$$T_{80}(i) = T_{80}(i-1) + k \cdot T_{80}(i-1) \tag{3.50}$$

Where T_{80} indicates temperature after combustion, k is a constant and **i** is counter for Mach number step.
Initial condition of this model have to be decided in different way as before: initial T_{80} for $M_0 = 4$ and k must be chosen to avoid excessive and unreal temperature after combustion values.

3.2.4 DMR Input Data

[21, 23]As shown before, dual-dome ramjet cycle requires different and various kind of input data, depending on model chosen. The most critical ones are reported and explained in this section.

- **Spillage Effect**

  CIRA has computed detailed CFD simulations on STRATOFLY MR3 intake, varying leading edge rounding, Mach number and angle of attack. Results show decreasing of air intake capturing efficiency with decreasing Mach number, this being due to the non-impingement of shock wave on the crotch; furthermore, the best rounding of leading edge is found as the one that minimize air mass and pressure losses. Total intake air mass flow losses are grouped in spillage effect.

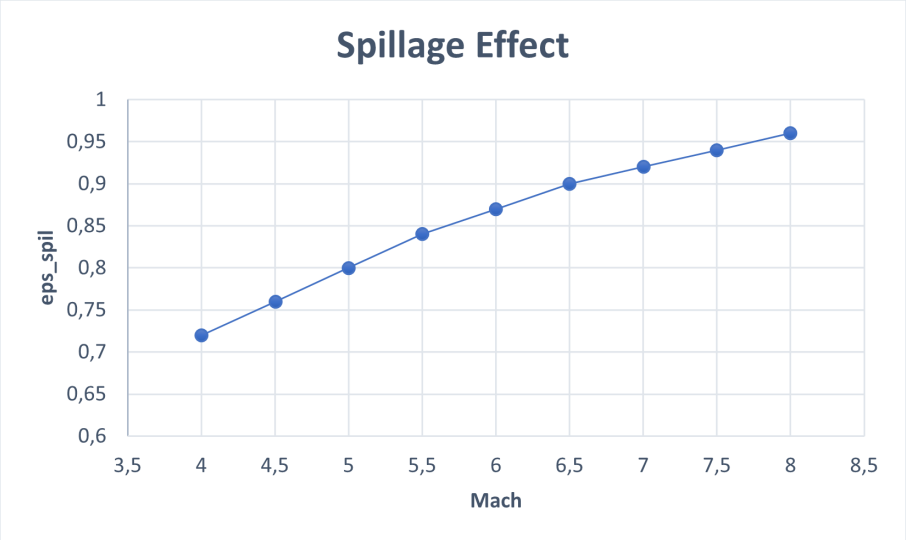

Figure 3.11. Spillage effect on STRATOFLY MR3

Figure 3.11 shows that spillage of mass flow reaches the minimum value at $M_0 = 8$ (corresponding to maximum value of $\varepsilon_s pil$), which is the design point.

- **Temperature After Combustion**

CIRA has also computed others simulations for the combustion temperature evaluation.
First one is the Jachimowski scheme, that "consists in 13 chemical species (including N, NO, NO2 and HNO) and 33 reversible, elementary, radical reactions and was specifically formulated for low-pressure (0.5; 1; 2 atm) supersonic combustion modelling in scramjet engines, operating at flight speeds up to Mach 25.
Instead, the Z22 kinetic mechanism, modified by inclusion of the three Zel'dovich NOx generation reactions, contains 13 chemical species and 25 reversible, radical, elementary reactions. It was developed and suitably optimized, through refinement of the kinetic rate parameters, for a more accurate prediction of experimental laminar burning velocities and ignition delay times at intermediate-low temperatures and elevated pressures (up to about 0.5 MPa)."[1]

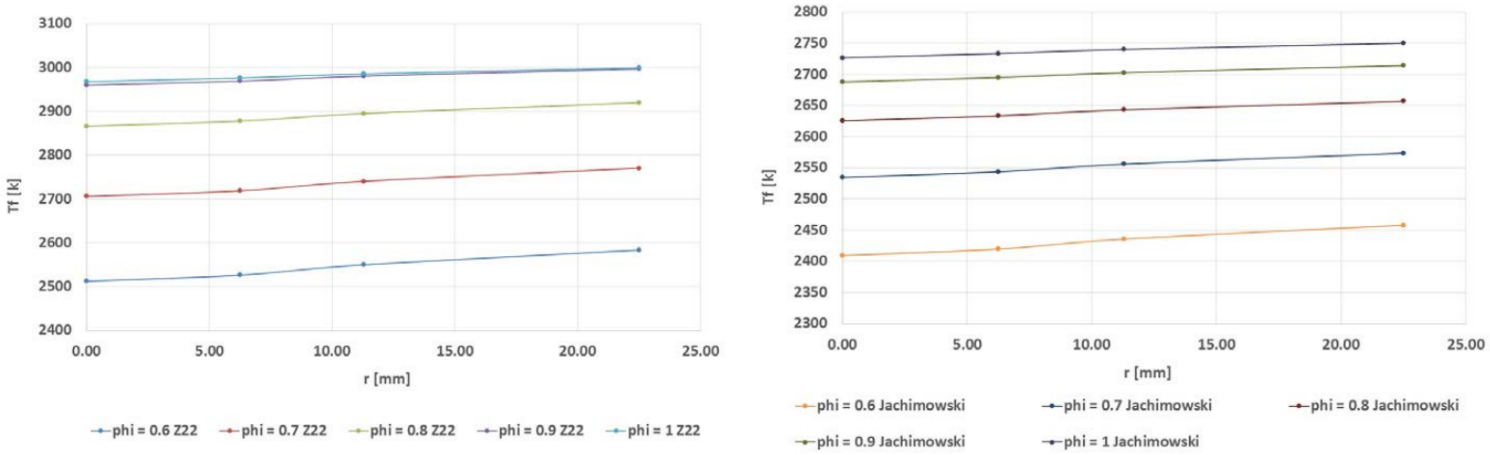

Figure 3.12. Z22 and Jachimowski mechanisms

Figure 3.12 reports temperature values varying intake leading edge rounding r and equivalent ratio $\phi = \frac{f}{f_{st}}$.

[1]P. Roncioni, M. Marini, G. Saccone, *D32 – WP3.4 Interim Report. Stratospheric Flying Opportunities for High-Speed Propulsion Concepts*, CIRA S.c.p.A., 2019

- **Intake Pressure Losses**

  CFD simulations by CIRA have also been useful to calculate pressure recovery factor *PRF*, that is the previous pneumatic intake efficiency ε_d; for STRATOFLY MR3, CFD results indicate that the value 11.3 mm of leading edge rounding is the more feasible solution at $M_0 = 8$.

The following values are utilised for simulations of STRATOFLY MR3 dual-mode ramjet.

COEFFICIENT	**VALUE**
Liquid Hydrogen	
Heats of reaction, H_i	*120.9 [MJ/kg]*
Stoichiometric fuel ratio, f_{st}	*0.029*
Combusted gases adiabatic expansion coefficient, γ'	*1.33*
Combusted gases specific heat, c'_p	*1900 [J/(kg*K)]*
Simple Ramjet Model	
Intake area, A_{10}	*37.7 [m^2]*
Pneumatic intake efficiency, ε_d	*0.35*
Pneumatic combustor efficiency, ε_b	*0.95*
Adiabatic combustor efficiency, η_b	*0.95*
Pneumatic nozzle efficiency, ε_n	*0.9*
Temperature after combustion Z22, T_{Z22}	*2970 [K]*
Temperature after combustion Jach, T_J	*2750 [K]*
Simple Ramjet Model with Temperature Variation	
Temperature after combustion, T_{80}	*2400 [K]*
Throttle parameters, k	*0.05*
Completed Ramjet Model	
Throat area, A_{80}	*4.9 [m^2]*
First nozzle area, A_{802}	*15.9 [m^2]*
Final nozzle area, A_{100}	*111.2 [m^2]*

Table 3.3. STRATOFLY MR3 Dual-Mode Ramjet input data

Every engine models need the previous parts included in Table 3.3.

3.2.5 DMR Propulsive Performances

From the specific impulse data calculated by the DMR tool by Steelant [18]. Thrust is being calculated by knowing the mass-flow rate being swallowed by the combustion chamber at a certain flight conditions and setting the equivalence ratio so that thrust can be obtained.

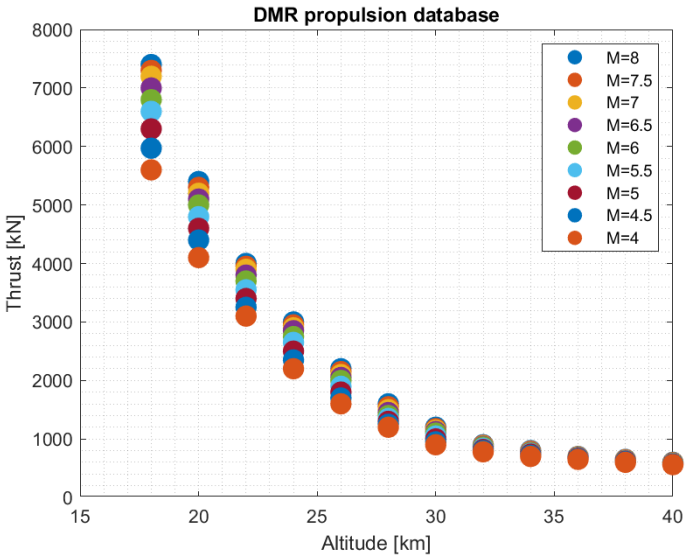

Figure 3.13. STRATOFLY MR3 DMR Propulsive database

Thrust data of the DMR propulsion database is plotted in 3.13 as a function of the Mach number and the flight altitude, while angle of attack and equivalent ratio are not varied.

- **Thrust**

$$T = \dot{m}_0 \cdot [(1 + f) \cdot w_e - u] \tag{3.51}$$

As for ATR and classic engine models, thrust is calculated as in Equation 3.51, but without term that consider nozzle adaptation $A_e \cdot (p_e - p_0)$.
The first graph of the simple ramjet model seems to be the most approximate the least correct when compared to the propulsion database. In this model, both end-of-combustion temperature values presented in the previous section were used: the Jachimowski mechanism up to Mach 7, and the Z22 mechanism for higher Mach numbers. This was done in order to ensure that the thrust reaches its maximum value for the highest speeds, as shown by the database;

if the temperature after combustion had remained constant, maximum thrust could have been observed for Mach less than 8.
Nevertheless, Simple Ramjet model turns out to be overestimated, both for the high Mach numbers and for the lower ones.
Thrust Equation 3.51 for Completed Ramjet model is modified.

$$T = 0.6 \cdot \dot{m}_0 \cdot [(1 + f) \cdot w_e - u] \tag{3.52}$$

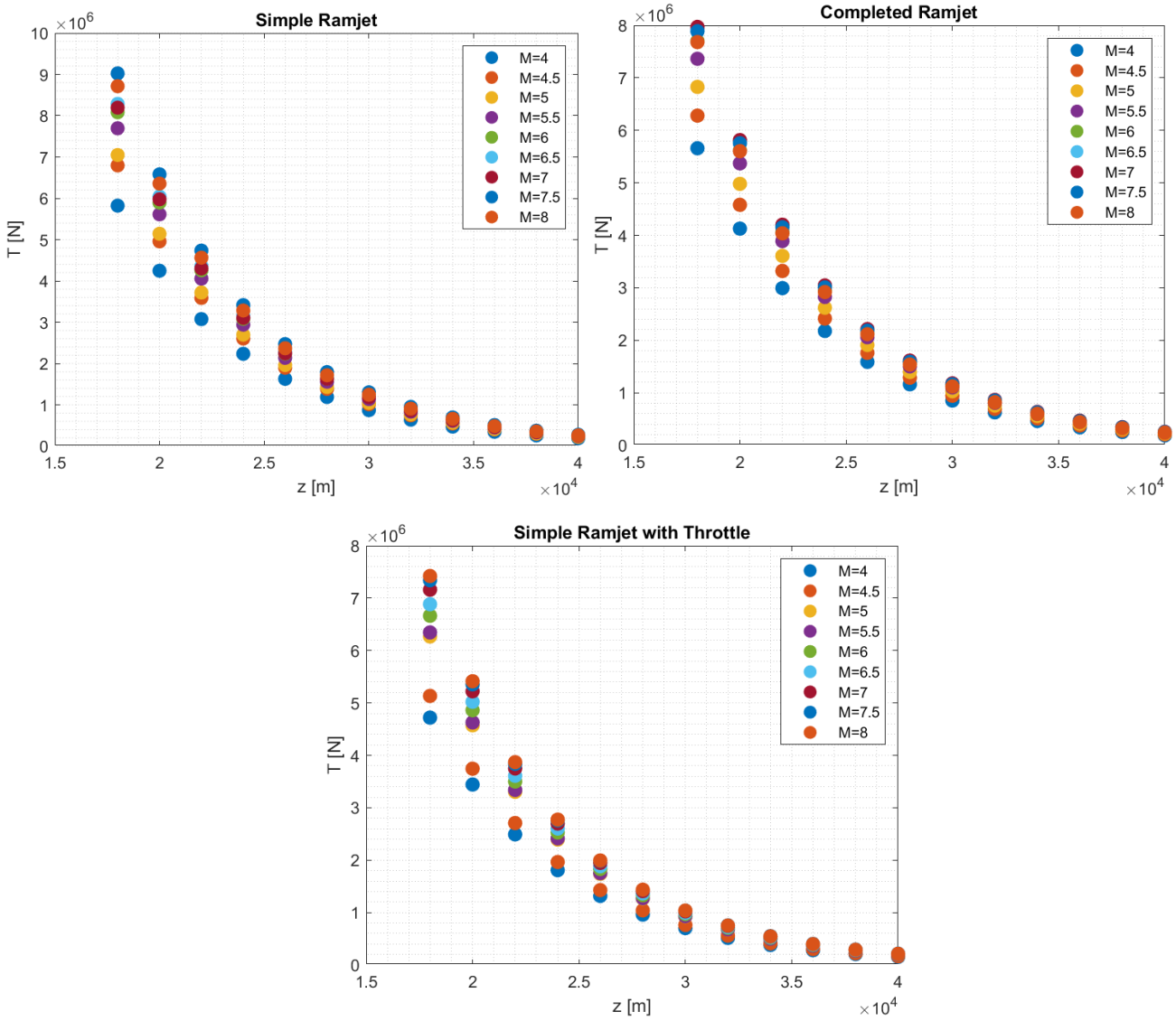

Figure 3.14. STRATOFLY MR3 Dual-Mode Ramjet Thrust

The constant multiplies argument to give a more similar results to the DMR database, otherwise model gives overestimated thrust value as in Figure 3.15. Constant can be considered as the representation of others mass-flow losses through the entire engine (not the spillage effect, which is considered in the appropriate coefficient).

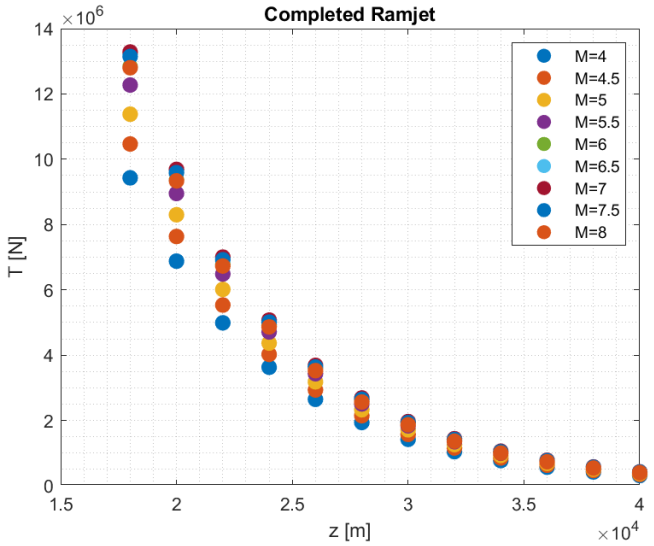

Figure 3.15. STRATOFLY MR3 DMR Completed model thrust without corrective constant

The last model (Simple Ramjet with Throttle) utilises Equation 3.51 and it seems to give the best results, compared with propulsive database (except for Mach numbers 4 and 4.5, where it is underestimated).

As for Air Turbo Rocket, differences between Dual-Mode Ramjet database and estimation can be calculated with Equation 3.53.

$$err = \frac{|T_{data} - T_{mod}|}{T_{data}} \tag{3.53}$$

Figure 3.16 shows similar features between all the models, with an increasing trend with altitude. Simple Ramjet with Throttle model has very close values with database, excepting for Mach numbers equal to 4 and 4.5, where thrust in underestimated. Completed Ramjet model shows better results then Simple Ramjet one, but it requests more input data.

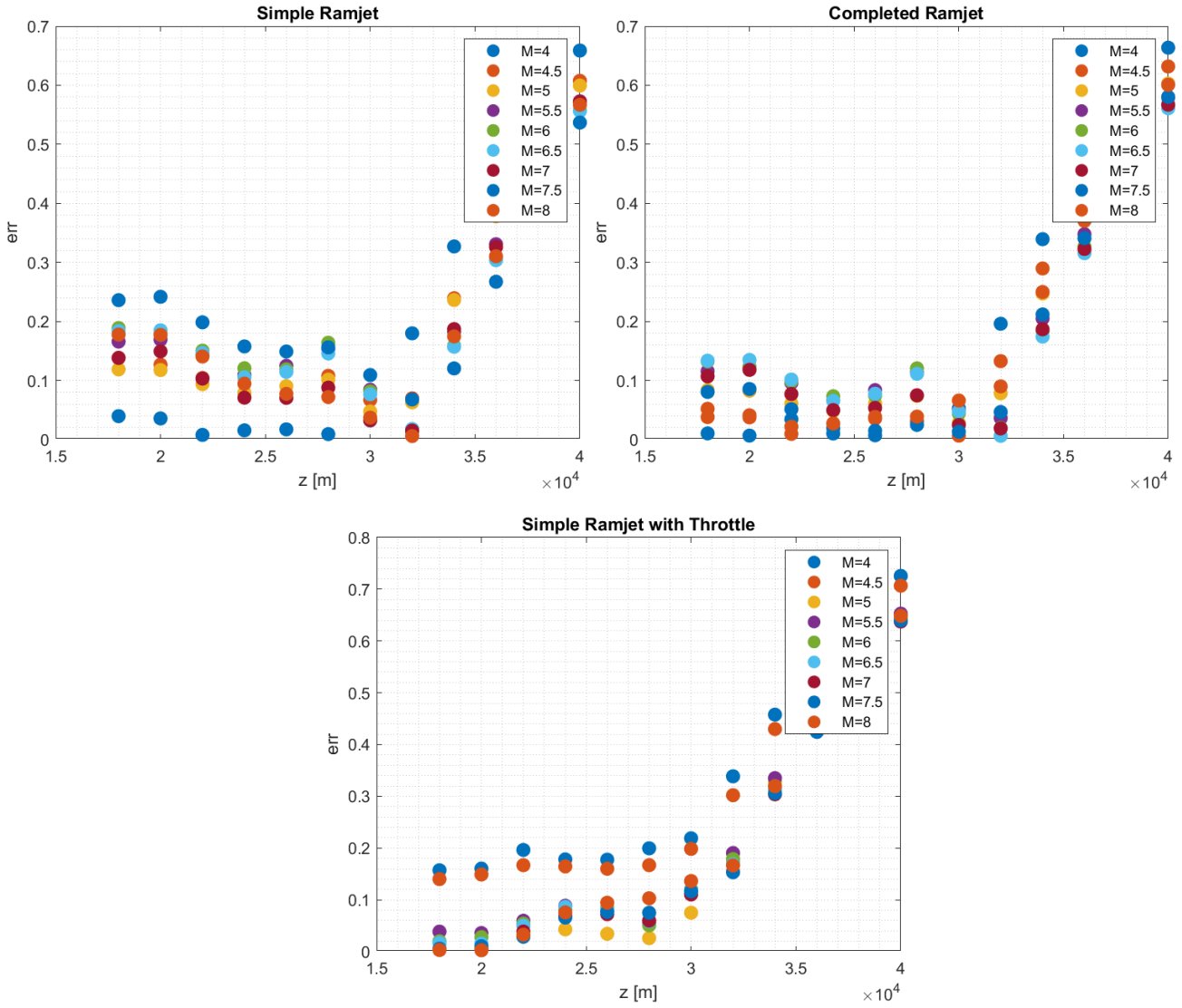

Figure 3.16. Error estimation between DMR database and different models

- **Specific Thrust**

As with the ATR propulsion database, also for the DMR the only reference data is thrust. Specific thrust and thrust specific fuel consumption can be calculated as in the previous cases, as reported in the Equations 3.54 and 3.18.

$$I_a = \frac{T}{\dot{m}_0} \tag{3.54}$$

The specific thrust (differently from ATR) follows a decreasing trend as the flight Mach increases. This occurs because most of the increase in thrust is due to the greater amount of air entering the engine, therefore to the higher flight speed; in addition, the combustion temperature remains constant or varies by small amounts compared to the average temperature (which is around 3000 K). As a result, the thrust increases, but more slowly than the intake air-mass flow.

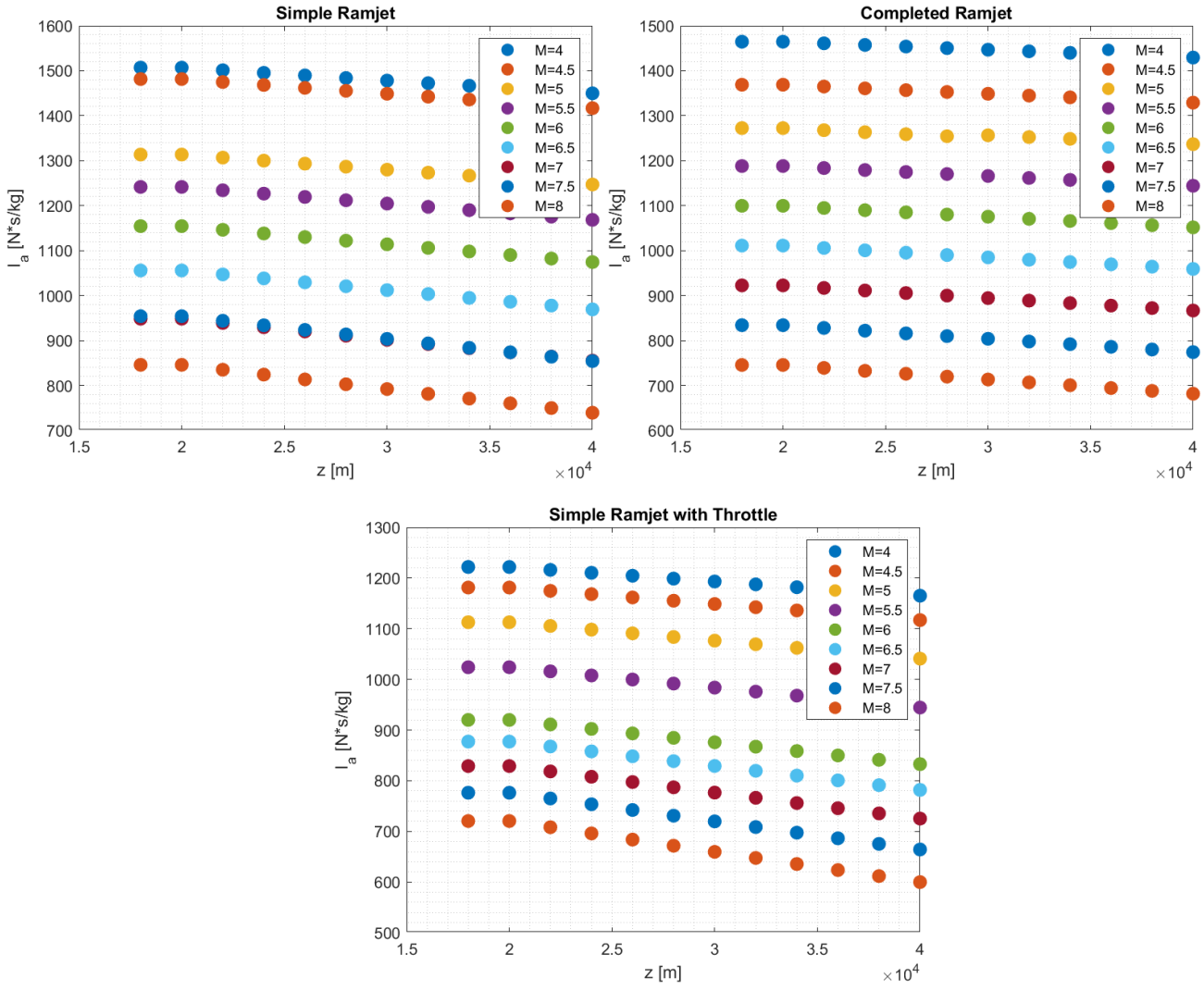

Figure 3.17. STRATOFLY MR3 Dual-Mode Ramjet Specific Thrust

- **Thrust Specific Fuel Consumption**

$$I_{sp} = \frac{\dot{m}_b}{T} \tag{3.55}$$

Similar trend of specific thrust can be followed in case of *TSFC*, whose increase is observed for grown Mach numbers; the reason is always linked to the faster growth of the intake air-mass flow rate, and therefore of the fuel flow rate.

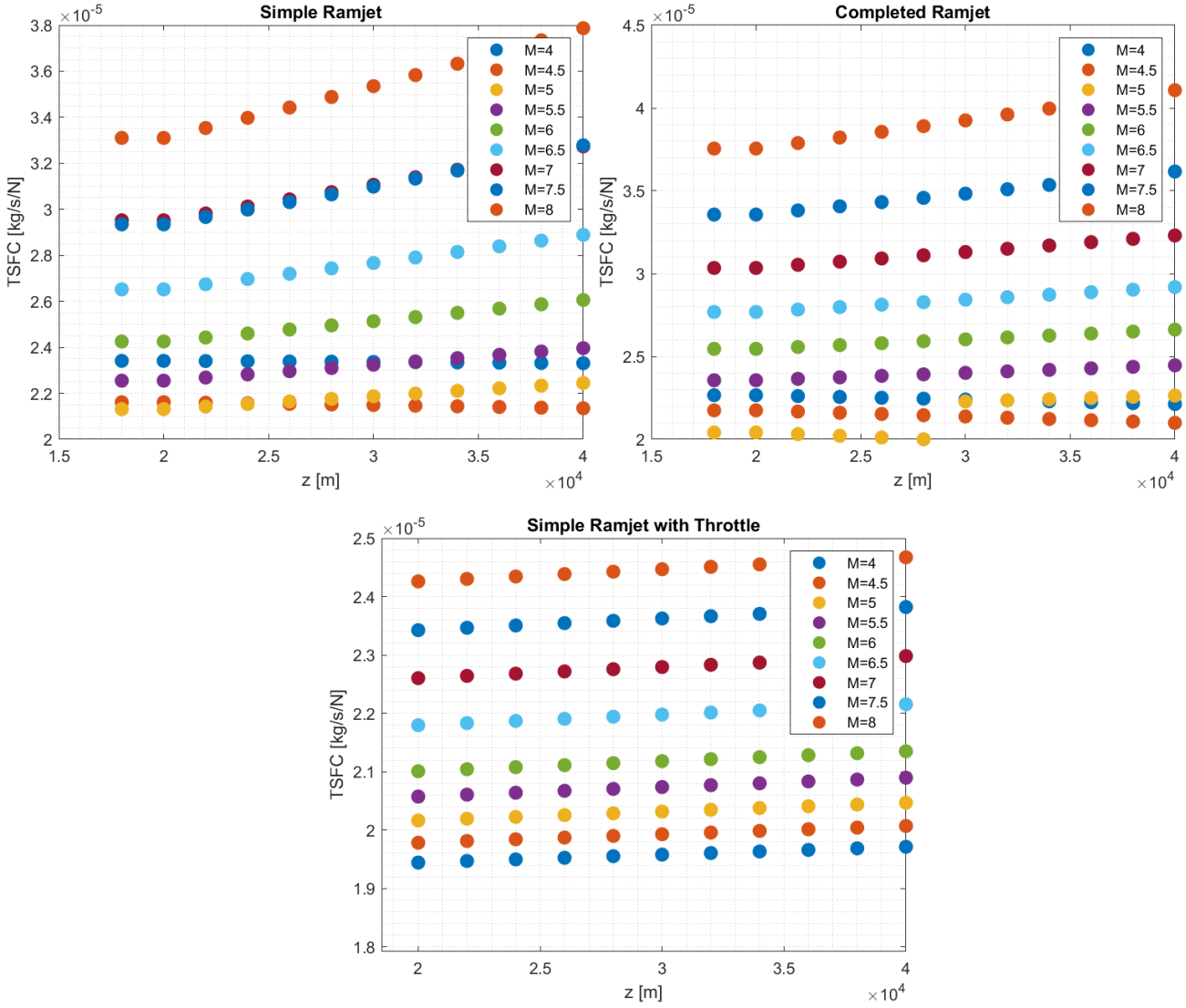

Figure 3.18. STRATOFLY MR3 Dual-Mode Ramjet Thrust Specific Fuel Consumption

Chapter 4

Graphical User Interface

The Graphical User Interface (GUI) is a type of user interface that permits to develop programmes that allow user to make effective and simple use of certain functions of a software program.
The last parts of thesis work concerns development of a GUI that permits user to obtain engine performance of an high-speed vehicle, varying some parameters; *MATLAB App Designer* is used to develop it.
Thanks to GUI development, propulsive estimation programme can be later add to ASTRID-H tool, which is a missing part of the software.
[24] *ASTRID-H* is a software tool developed at Politecnico di Torino to support the conceptual and preliminary design phases of high-speed vehicles. Based on the experience in the development of innovative methodologies to cope with complex and highly integrated aircraft, ASTRID-H has been developed to guide students, researchers and engineers through the very first phases of the design of high-speed vehicles. ASTRID-H supports the users to move from the statistical evaluation of the guess data and the identification of the design space to the geometrical characterization of the vehicle guaranteeing a proper integration of the main subsystems. The resulting implemented methodology allows the users to cope with complex multidisciplinary problems, which encompass a variety of interrelated disciplines and heterogeneous levels of fidelity.

4.1 GUI Architecture

In Figures 4.1, 4.2, 4.3 architecture of the GUI is reported.
First at all, user has to select engine to develop, between the classic thermodynamic engine (single-spool turbojet, twin-spool turbojet, turbofan or ramjet) and the hypersonic ones (Air Turbo Rocket or Dual-Mode Ramjet).
If a subsonic or supersonic engines is chosen, user has to insert the requested input. Atmosphere model described in Subsection 2.1 has been already loaded in every engine script; so, the necessary inputs regards each engine components, such as Overall Pressure Ratio, Turbine Inlet Temperature, adiabatic, pneumatic and mechanic efficiencies, intake and exit nozzle areas. Some air and fuel data have to be insert, so that user can also chose propellant properties. All the inputs necessary for these engine class are reported in Figure 4.1. For single-spool and twin-spool turbojet, afterburner data can be inserted only if it is selected by user.
For ATR and DMR, differently from before, not all the inputs can be changed by user, but only the red ones in Figures 4.2 and 4.3. The reason why not every input data can be modified by user is due to specificity of the built models; furthermore, as the models are validated on a single category of aircraft, changing too much data could make the results unreliable.
ATR requires some engine data, intake geometry (for the most complete model also nozzle one) and air-fuel ratio; if the propellant-cycle is present in model selected, compression ratio of of dedicated pump is requested. End of combustion temperature can be inserted if it is known. No input data about efficiencies are requested for Air Turbo Rocket.
DMR cycle requires, in addition to the classic values already found in ATR, intake efficiency, both for low and high speeds. The coefficient for the spillage effect cannot be modified by user, as it is derived from detailed CFD analyses.
For the Simple Ramjet with Throttle model Equation 3.50, that represents throttle variation with temperature after combustion, can be modified, varying both starting combustion temperature and constant multiplying value.
Inside the GUI, for each input data requested from the user, programme suggests the values relative to the engines analysed in the previous chapters: for the DMR and ATR, the data relative to the *STRATOFLY MR3* are suggested, for the single-spool and twin-spool turbojets respectively the data of the *J85 GE* and the *Olympus 593*, for the turbofan the data of *JT9D*; in the case of simple ramjet the suggested data are not those relative to a specific engine, but refer to the average values observable for this class.
Results shown regard thrust, specific thrust and TSFC, varying altitude and Mach number. Both for ATR and DMR models, a comparison of thrust trend of all the models can be observed; certainly, every input data can be inserted by user.

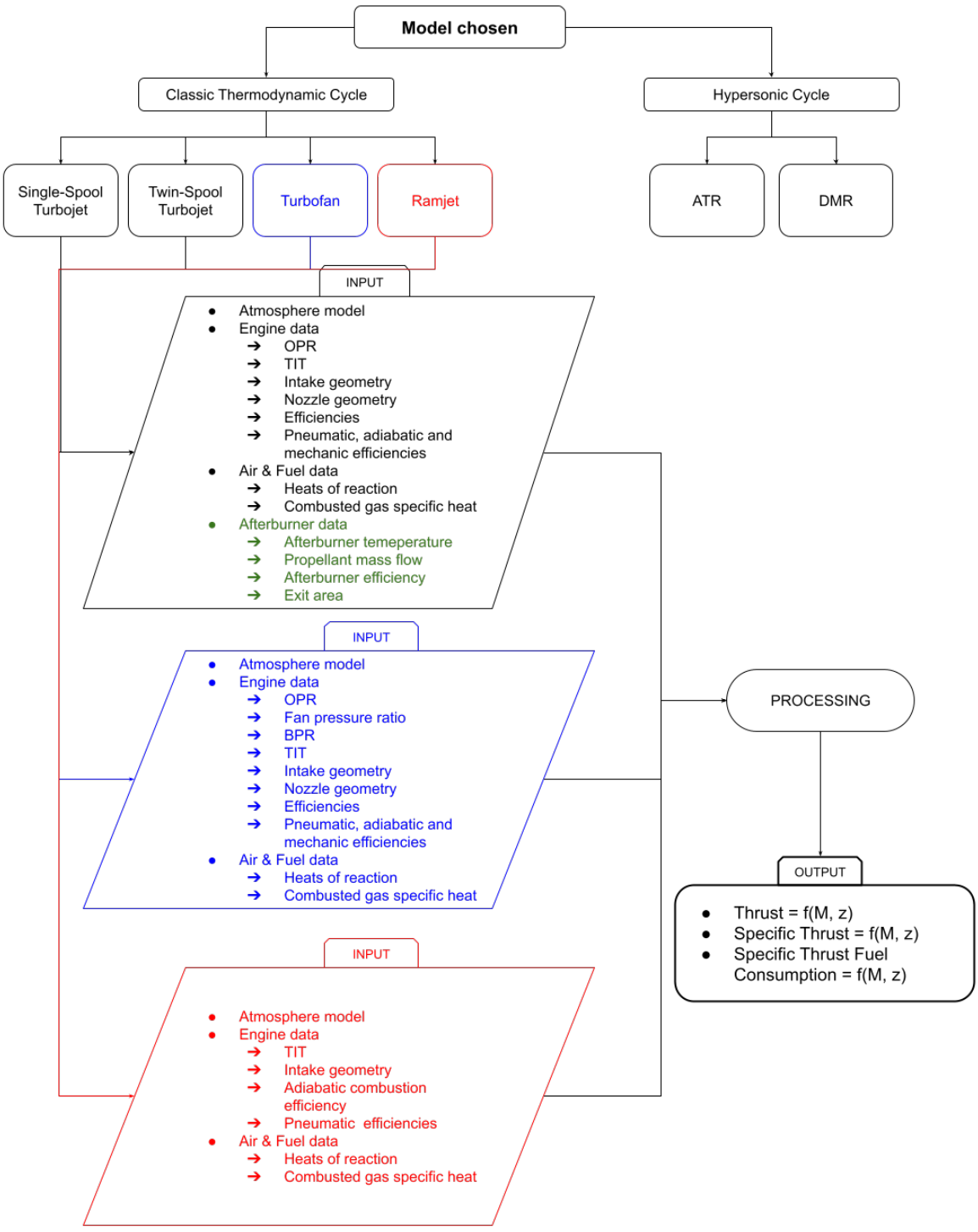

Figure 4.1. Graphical User Interface Flowchart

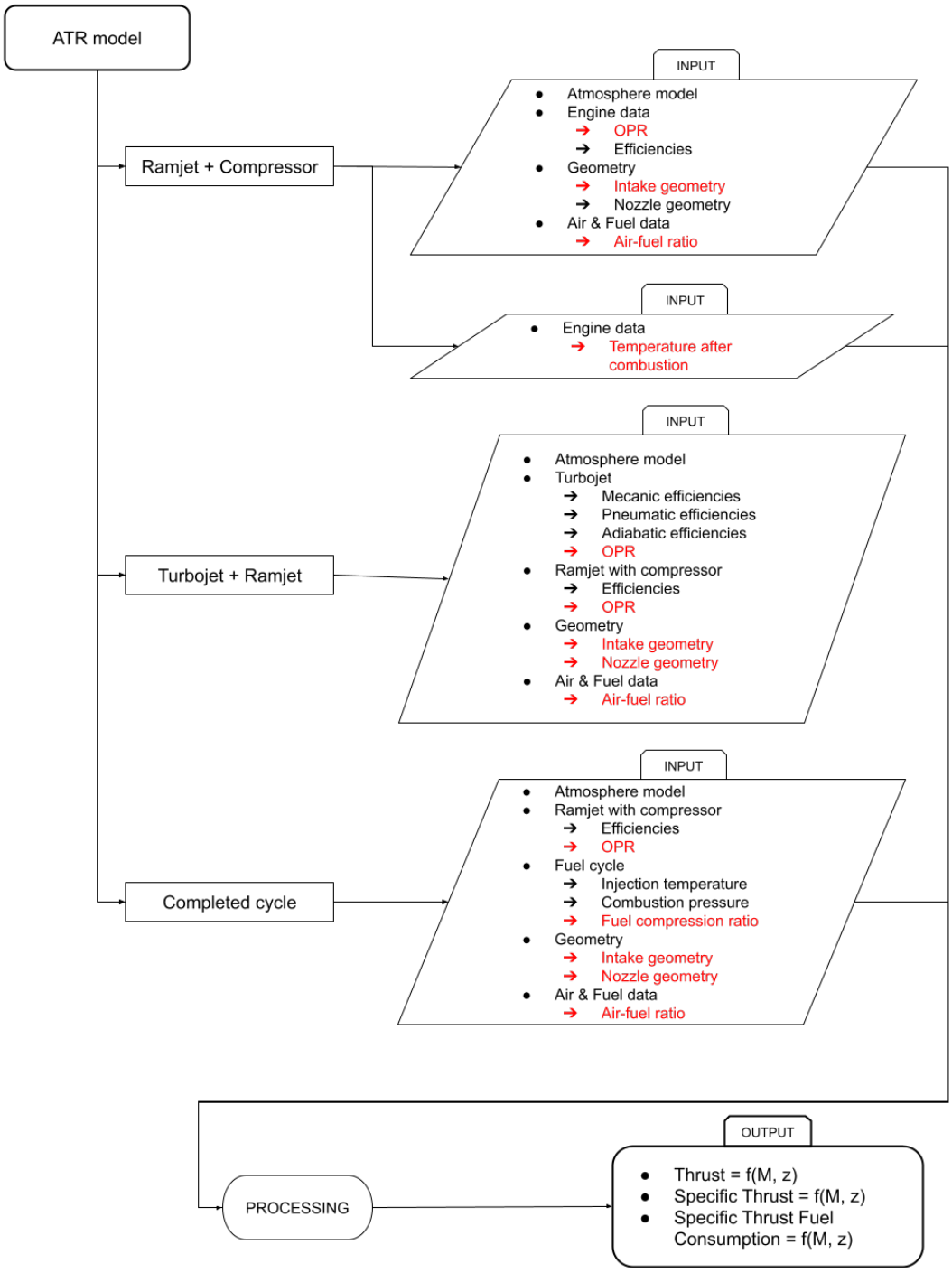

Figure 4.2. Graphical User Interface ATR Flowchart

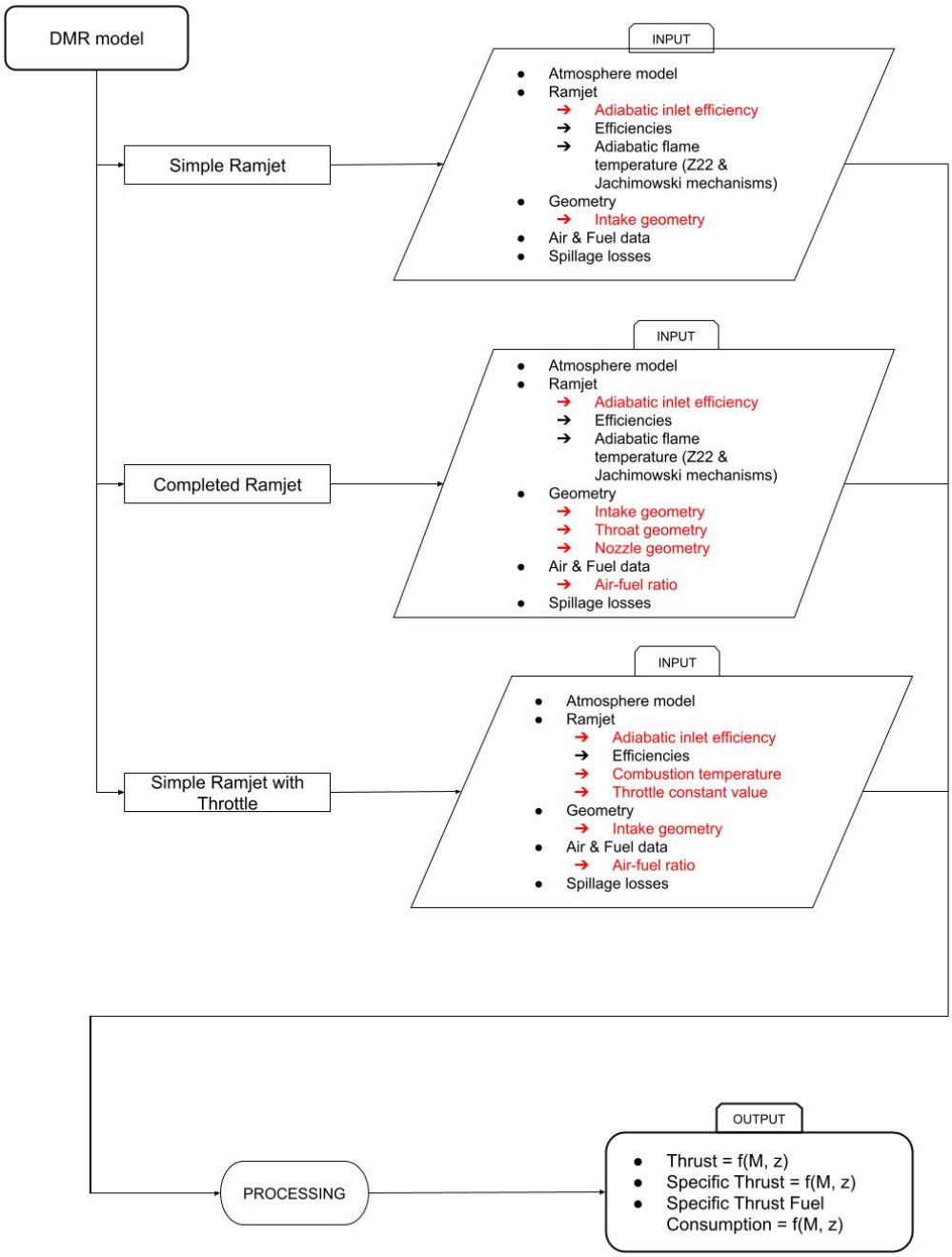

Figure 4.3. Graphical User Interface DMR Flowchart

4.2 User Guide (Examples)

Starting page of GUI permits selection of the class of engine; choose can be done between classic thermodynamic cycle of subsonic and supersonic aircraft (turbojets, turbofan and ramjet) and hypersonic engine (ATR and DMR) as in Figure 4.4. Selecting one of the engine, 'Start Analysis' button will become enable.

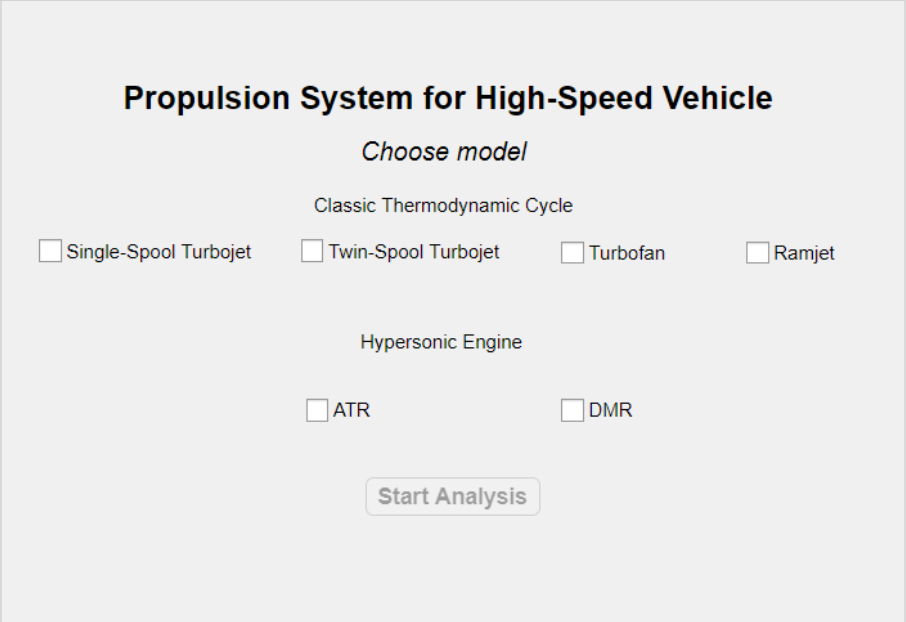

Figure 4.4. Graphical User Interface starting page

4.2.1 Single-Spool Turbojet

If Single-Spool Turbojet is selected between engine, pressing 'Start Analysis' button, user will be sent to turbojet input page (Figure 4.5. Then, user has to decide if afterburner is present or not. Selecting 'Classic Turbojet' (no afterburner), only Engine data and Fuel data are enabled. User must insert every values of enabled field; pressing '?' button, suggested value can be read (Figure 4.6).
The last button, which is present also in other pages, is 'Exit': it will sent user to the first programme page.

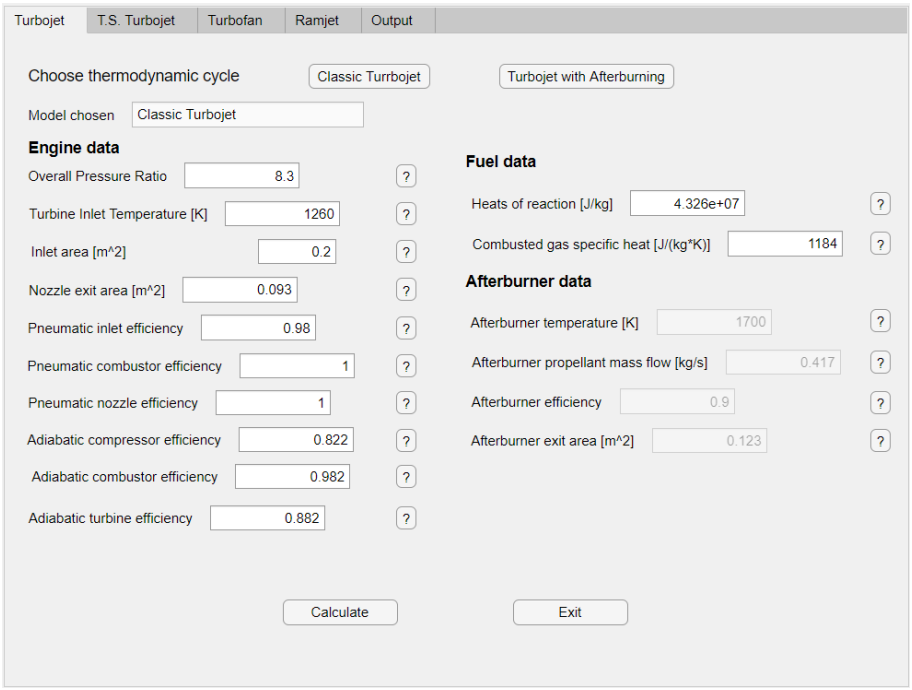

Figure 4.5. Graphical User Interface single-spool turbojet input

Pressing 'Calculate' button, user will be sent to output page (4.7), where it is possible to choose the output to plot in the graph (thrust, specific thrust and TSFC). Selecting 'Thrust' and pressing 'Plot', result is shown as function of altitude and Mach number. Thrust maximum value is reached between Mach 1.2 and 1.4, as expected from classic turbojet model; after these Mach values, performance starts to decrease, due to fixed Turbine Inlet Temperature.

Figure 4.6. Graphical User Interface TIT suggested value for turbojet

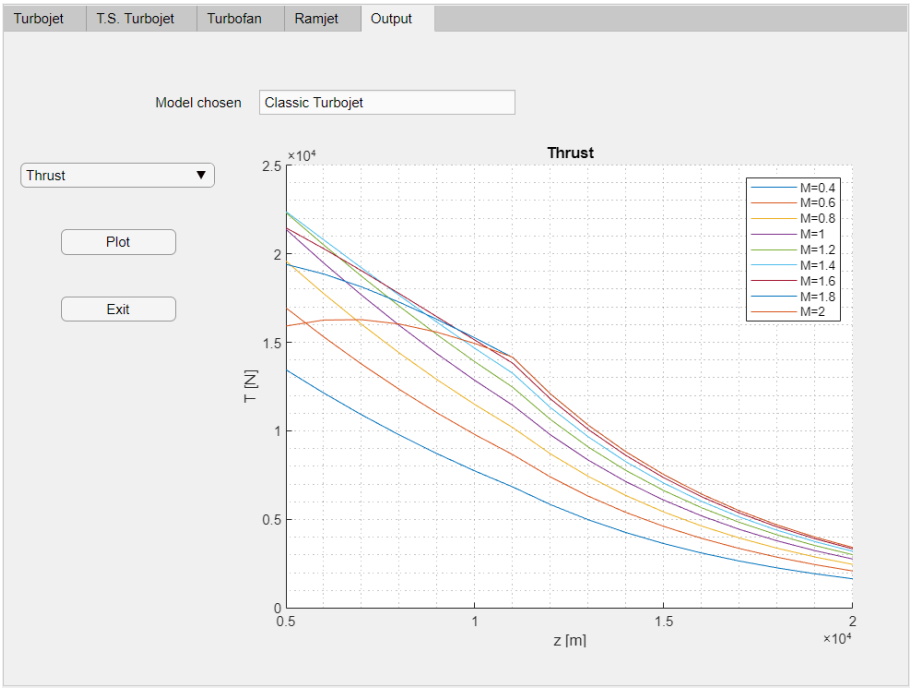

Figure 4.7. Graphical User Interface single-spool turbojet results

In single-spool and twin-spool turbojets GUI there is possibility of adding afterburning phase to a classic thermodynamic cycle, pressing 'Turbojet with Afterburner' button. In this way afterburner input data are enabled and can be inserted by user (Figure 4.9).

Figure 4.6 shows results of single-spool with afterburner; comparing with Figure 4.9, greater thrust values are achieved, as excepted, and maximum performance are reached for Mach 2.

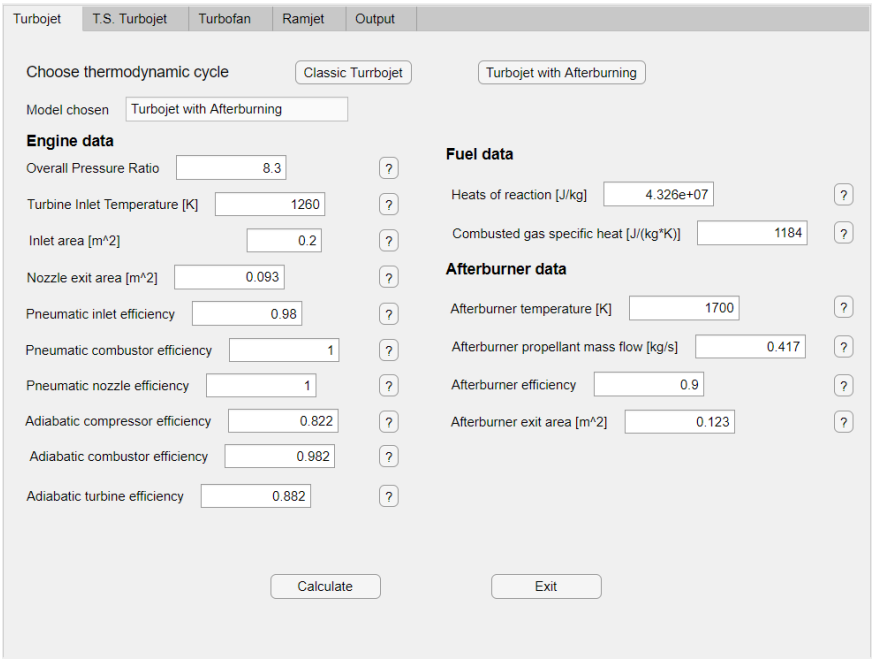

Figure 4.8. Graphical User Interface single-spool turbojet with afterburner input

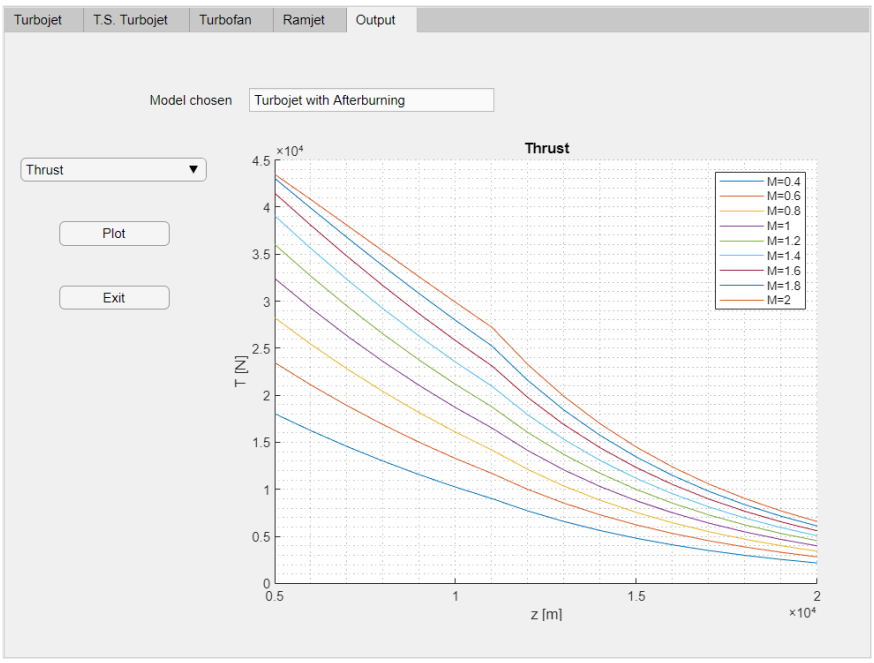

Figure 4.9. Graphical User Interface single-spool turbojet with afterburner results

4.2.2 Dual-Mode Ramjet

For high-speed vehicle GUI, ATR and DMR are developed; user can choose between all the models presented in Chapter 3.

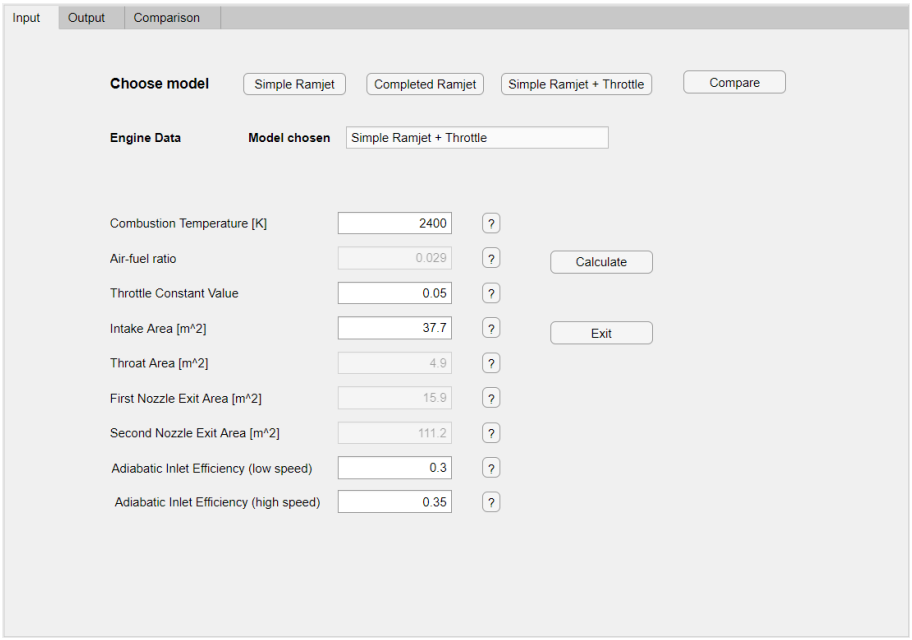

Figure 4.10. Graphical User Interface DMR input

Dual-Mode Ramjet interface permits to evaluate Simple Ramjet, Completed Ramjet and Simple Ramjet with Throttle models, plus a comparison of thrust performance.
Selecting 'Simple Ramjet + Throttle', input data of Figure 4.10 are enabled. As before, pressing 'Calculate' button, user will be sent to output page.

Figure 4.11 shows thrust performance of the selected model, already explained in Chapter 3.
Other performances can also be plotted in the graph, selecting them through the drop down box. If 'Specific Thrust' choice is selected, magnitude will be plotted in the graph, as in Figure 4.12.

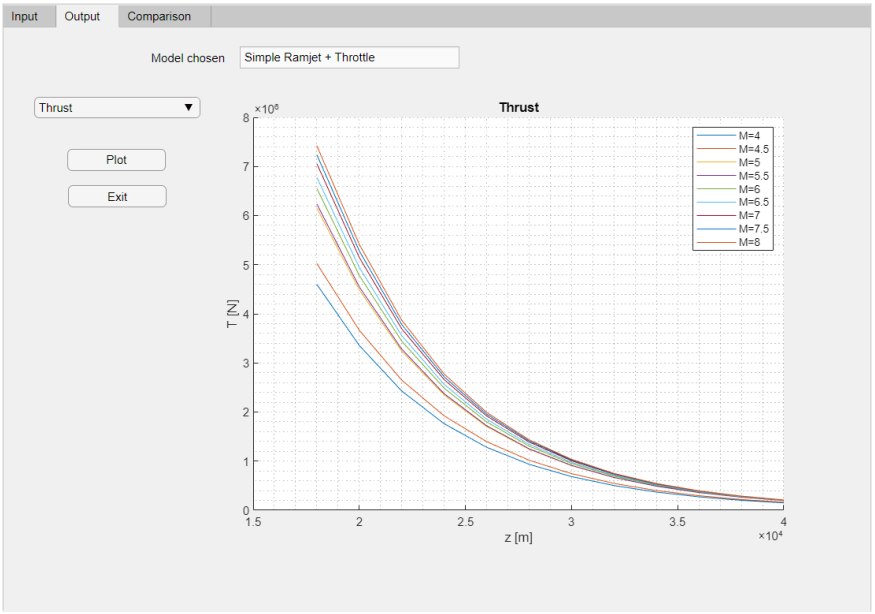

Figure 4.11. Graphical User Interface DMR thrust results

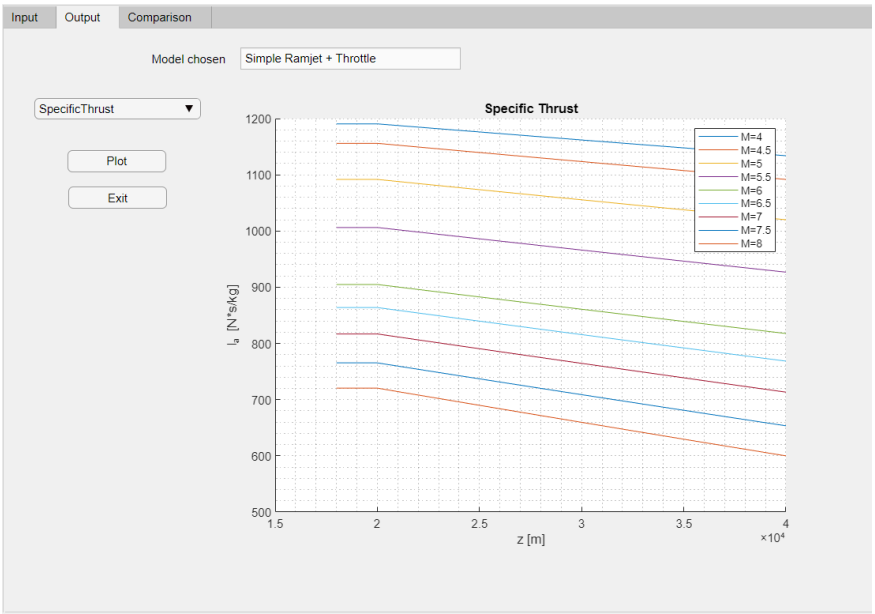

Figure 4.12. Graphical User Interface DMR TSFC results

4.2.3 Air Turbo Rocket

Air Turbo Rocket analysis permits evaluation of engine performances through models presented before: 'Ramjet + Compressor (Temperature known or unknown)', 'Turbojet + Ramjet' and 'Completed' one.
In case user selects 'Ramjet + Compressor' model, another choice has to be done before data input insertion: end of combustion temperature can be inserted manually (pressing 'Temperature known') or it can be calculated by programme (pressing 'Temperature unknown').

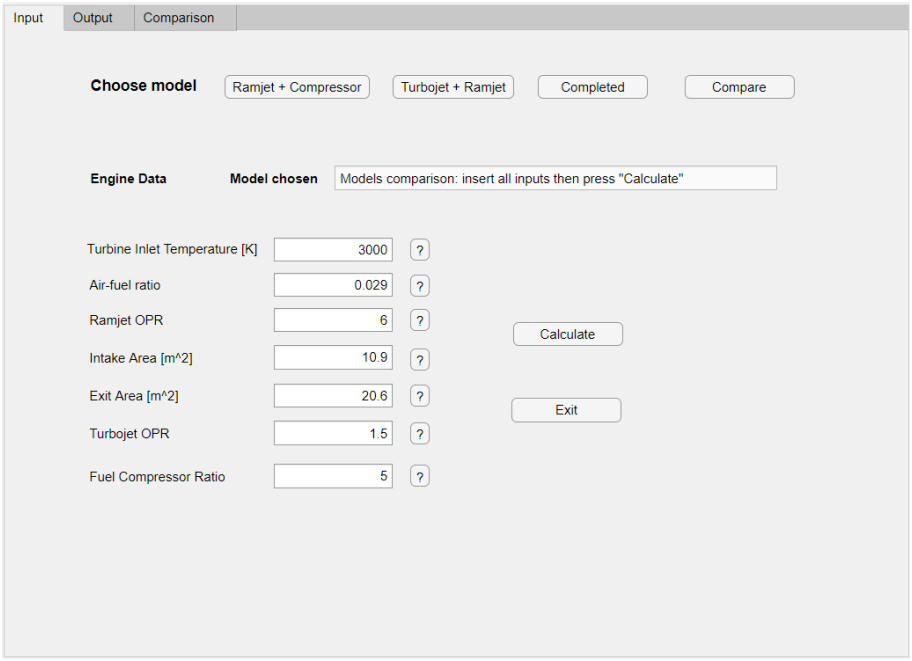

Figure 4.13. Graphical User Interface ATR input

In addition to the individual models for the ATR, as well as for the DMR, it is possible to compare the thrust of each programme in order to give user the possibility to choose the most suitable model for his purposes. This function is carried out by the 'Compare' button, which requests user to enter all inputs (Figure 4.13).
After input data insertion, user has to click on 'Calculate' button and he will be sent to 'Comparison' tab, where thrust performance of every models is plotted, as in Figure 4.14.

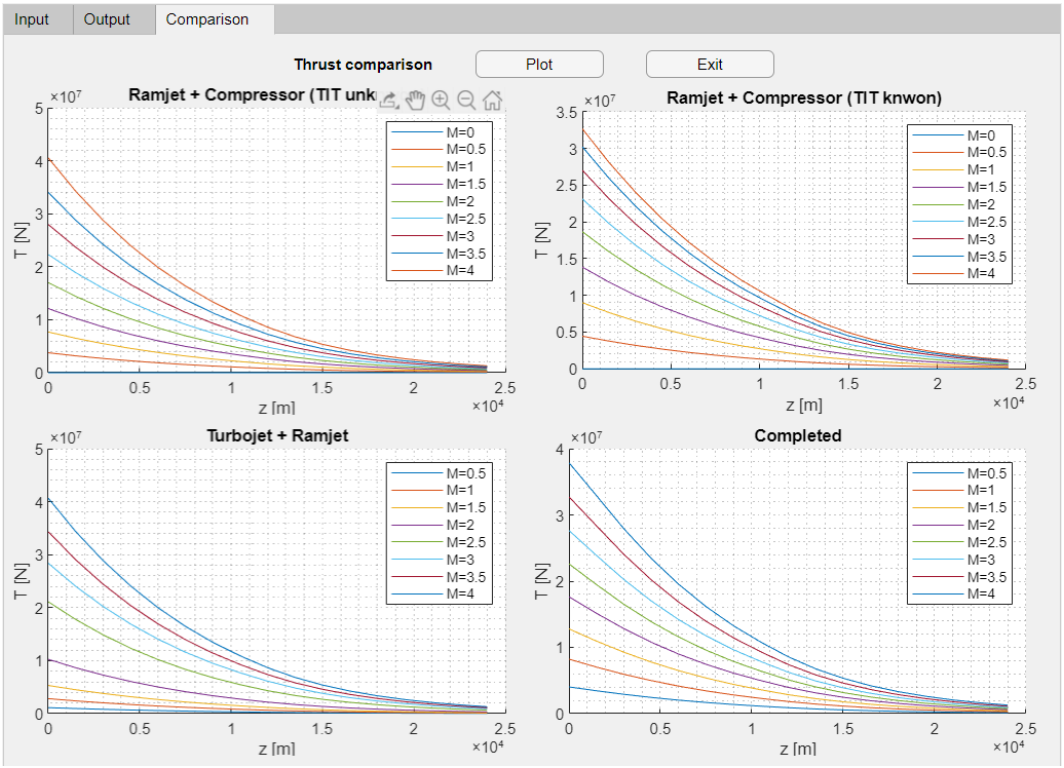

Figure 4.14. Graphical User Interface ATR comparing results

Chapter 5

Conclusions

Thesis work focused the attention on the conceptual design of propulsion system. The dissertation addressed two main areas related to aviation propulsion: existing thermodynamic cycles and the most innovative ones.
In the first part, the classic engine categories (single-spool turbojet, twin-spool turbojet, turbofan and ramjet) for subsonic and supersonic flight were analysed; these models were implemented on *MATLAB* software and validated with existing engine data. For hypersonic flight, several solutions were developed to calculate the performance of the Air Turbo Rocket and Dual-Mode Ramjet engines.
Further work would concern hypersonic engines; the analyses carried out to date have been based on STRATOFLY MR3 aircraft, in particular on ATR and DMR. In literature, there are other hypersonic aircraft projects that use engines similar to those of the STRATOFLY, or more different propulsion systems (such as the SABRE and the Scimitar). The development of these models would extend the possibilities of calculating engines performance, that are very different from those analysed. The main problem in doing so would be the search for reliable data, which is very complicated for this aircraft category.
New engines will be added in Graphical User Interface introduced in Chapter 4. The same tool could be also integrated in *ASTRID-H*; this solution can guarantee a more completed preliminary dimensioning, including in the same software various vehicle aspects. In this way, the aim of evaluating the propulsive performance of hypersonic aircraft within the conceptual design phase would be completely achieved.

Bibliography

[1] Jack D. Mattingly, William H. Heiser, David T. Pratt, *Aircraft Engine Design*, American Institute of Aeronautics and Astronautic, Second Edition

[2] H. I. H. Saravanamuttoo, G. F. C. Rogers, H. Cohen, *GAS TURBINE THEORY*, PEARSON

[3] Charlie Svoboda, *Turbofan engine database as a preliminary design tool*, Department of Aerospace Engineering, The University of Kansas, 2004 Learned Hall, Lawrence, KS 66045, USA

[4] E.T. Curran, S.N.B. Murthy, *Scramjet Propulsion*, Volume 189 PROGRESS IN ASTRONAUTICS AND AERONAUTICS

[5] F. Nasuti, D. Lentini, F. Gamma, *Dispense del Corso di Propulsione Aerospaziale*, Università degli Studi di Roma "La Sapienza", 2004

[6] Ing. F. Nicolosi, *Modulo di PRESTAZIONI, Corso di Laurea in Ingegneria Aerospaziale*

[7] L. Casalino, D. Pastrone, *Dispense del Corso di Fondamenti di Macchine e Propulsione*, Politecnico di Torino, 2017

[8] D. Pastrone, *Dispense del Corso di Motori per Aeromobili*, Politecnico di Torino, 2018

[9] Philip G. Hill, Carl R. Peterson, *MECHANICS AND THERMODYNAMICS OF PROPULSION*, Second Edition, PEARSON

[10] L. Trainelli, *Lezioni di Meccanica del Volo*, 2011

[11] G. Stiuso, *Tecnica di simulazione numerica delle prestazioni stazionarie e transitorie di turbomotori*, Politecnico di Torino, 2019

[12] European Union Aviation Safety Agency (EASA), *ICAO Aircraft Engine Emissions Databank*, 2020

[13] Amit Batra, *Aerothermal Flow Path Analysis and Design of a Hypersonic Propulsion Unit*, Department of Aerospace Engineering Indian Institute of Technology, Bombay, 2002

[14] Victor Fernàndez-Villacé *Simulation, Design and Analysis of Air-Breathing Combined-Cycle Engine for High-Speed Propulsion*, Escuela Técnica Superior de Ingenieros Aeronàuticos, 2013

[15] J.M.A. Longo, R. Dittrich, D. Banuti, M. Sippel, J. Klevanski, U. Atanassov, *Concept Study for a Mach 6 Transport Aircraft*, German Aerospace Center (DLR), Germany, 2014

[16] Neil Murray, Johan Steelant, *Methodologies involved in the Design of LAPCAT-MR1: a Hypersonic Cruise Passenger Vehicle*, American Institute of Aeronautics and Astronautics, 2009

[17] V. Fernàndez–Villacé, G. Paniagua, J. Steelant, *Installed performance of an air turbo–rocket expander engine during supersonic acceleration*, Space Propulsion, 2014

[18] T. Langener, J. Steelant, *Trajectory Analysis for the Updated LAPCAT-MR2.4 Waverider based Vehicle*, Long-Term Advanced Propulsion Concepts and Technologies II, 2013

[19] J. Steelant, R. Varvill, S. Defoor, K. Hannemann, M. Marini, *Achievements Obtained for Sustained Hypersonic Flight within the LAPCAT-II Project*, 20th AIAA International Space Planes and Hypersonic Systems and Technologies Conference, 2015

[20] J. Steelant, *LAPCAT: High-Speed Propulsion Technology*, ESA-ESTEC Division of Propulsion and Aerothermodynamics, 2008

[21] P. Roncioni, M. Marini, G. Saccone, *D32 – WP3.4 Interim Report. Stratospheric Flying Opportunities for High-Speed Propulsion Concepts*, CIRA S.c.p.A., 2019

[22] R. Fusaro, N. Viola, *Design and integration of a cryogenic propellant subsystem for the hypersonic STRATOFLY MR3 Vehicle*, Politecnico di Torino, 2019

[23] Nicole Viola, Roberta Fusaro and Oscar Gori, *STRATOFLY MR3 – how to reduce the environmental impact of high-speed transportation*, Institute of Air Transportation Systems, Hamburg, Germany

[24] Davide Ferretto, Roberta Fusaro and Nicole Viola*A conceptual design tool to support high-speed vehicle design*, Politecnico di Torino, Torino, Italy